NATIONAL ADVISORY COMMITTEE FOR AERONAUTICS

TECHNICAL NOTE 3505

AN EXPERIMENTAL INVESTIGATION OF REGIONS OF SEPARATED LAMINAR FLOW

By Donald E. Gault

Ames Aeronautical Laboratory
Moffett Field, Calif.

Washington
September 1955

NATIONAL ADVISORY COMMITTEE FOR AERONAUTICS

TECHNICAL NOTE 3505

AN EXPERIMENTAL INVESTIGATION OF REGIONS OF SEPARATED LAMINAR FLOW

By Donald E. Gault

SUMMARY

Results are presented from an investigation of regions of separated flow caused by separation of the laminar boundary layer (laminar-separation "bubbles"). The investigation was undertaken to obtain measurements which would define a large number of these bubbles for a wide range of Reynolds numbers and pressure gradients. In this manner, existing physical interpretations of the flow along a bubble could be studied in greater detail than in the past and, at the same time, it was hoped that the data would provide further insight into the conditions which control the occurrence and extent of a bubble.

Total- and static-pressure surveys, hot-wire-anemometer observations, and detailed pressure-distribution and liquid-film measurements were made in regions of separated flow on two airfoils. The measurements were obtained for a wide range of angles of attack and for Reynolds numbers from 1.5 million to 10 million. A limited investigation of the effects of an increase in the free-stream turbulence also was made.

The conditions which determine whether or not a bubble will form after the occurrence of laminar separation were not ascertained. However, apparently a necessary condition for the occurrence of a bubble, although not a sufficient condition, is that the boundary-layer Reynolds number at the position of laminar separation must be greater than a certain critical value; this critical value, as evaluated by previous investigators, is of the order of 500, based on the boundary-layer displacement thickness. When a bubble is formed the extent of separated laminar flow, near the leading edge of an airfoil, is approximately 75 to 85 percent of the total extent of separated flow and depends primarily on both a measure of the local Reynolds number of the laminar boundary-layer flow and on the boundary-layer thickness at the position of laminar separation. There also appears to be some relationship between the extent of separated laminar flow and the pressure distribution. An increase in the free-stream turbulence reduces the extent of separated flow in a manner somewhat analogous to an increase in the Reynolds number. It was found that the position of transition in a bubble can be ascertained with considerable accuracy from detailed surface pressure-distribution measurements.

INTRODUCTION

Observations of local regions of separated flow have been reported by a number of investigators in the past (refs. 1 to 9). Briefly, these regions of separated flow originate when a laminar boundary layer separates from a surface. Transition to turbulent flow takes place in the detached boundary layer a short distance downstream from separation. The flow then becomes re-established on the surface and passes on downstream with a turbulent boundary layer. The region underlying the separated flow, between the limits of separation and reattachment, has become commonly termed the "laminar-separation bubble."

These regions of separated flow are best known because of their occurrence on the upper surfaces of airfoils just behind the leading-edge pressure peaks for large angles of attack (e.g., refs. 1, 2, 6, and 7). Under such conditions, they are, as discussed by McCullough and Gault in reference 10, an important factor in determining the boundary-layer and stalling characteristics of airfoils covering a wide range of thickness ratios. In addition, Bursnall and Loftin (ref. 8) have observed these regions near midchord on comparatively thick airfoils for angles of attack near 0°. However, the occurrence and importance of laminar-separation bubbles are not necessarily restricted to the flow about airfoils. Another investigation reported by Bursnall and Loftin (ref. 11) and some unpublished liquid-film and boundary-layer measurements obtained in connection with reference 12 by Delany and Sorensen show that the bubble flow can appear on circular cylinders for Reynolds numbers in the supercritical range. Moreover, although the present report is concerned only with subsonic conditions, regions of separated flow initiated by laminar separation have been observed in supersonic flow (e.g., Ackeret, Fieldmann, and Rott in ref. 13).

The formation of a bubble is, therefore, fairly common and may or may not accompany transition from laminar to turbulent flow. It is known that a laminar boundary layer will separate from the surface under the influence of a sufficiently large adverse pressure gradient. For a given distribution of pressure the position of separation is theoretically fixed at a particular point along the surface. In contrast, transition depends on many variables including Reynolds number, surface roughness, and free-stream turbulence as well as pressure gradient; an increase in any of these variables will, in general, cause transition to move upstream. As a result, under some conditions, it is possible for transition to preclude laminar separation and the formation of a bubble by originating upstream of the point at which the laminar flow would detach from the surface. For other conditions, however, separation can occur and transition will take place in the detached flow. The occurrence of separation, although a necessary condition, of course, is not a sufficient condition for the formation of a bubble. In some circumstances the flow does not reattach to the surface and form a bubble but continues downstream in the separated state to form a large turbulent wake. If the surface extends

downstream a sufficient distance, this turbulent wake may eventually reattach to the surface and form a region of separated flow which is, in general, much larger than a bubble. However, such regions of separated flow appear to be quite different than the bubble type of flow and, hence, are not considered herein (see ref. 10).

Jones recognized the occurrence of laminar-separation bubbles in references 1 and 2. Since then several investigators have attempted to define, in quantitative terms, the conditions under which these regions are formed and the variables which control the extent of separated flow when a bubble is formed (von Doenhoff in ref. 3; Jacobs and von Doenhoff in ref. 4; Bursnall and Loftin in ref. 8; Maekawa and Atsumi in ref. 9; Owen and Klanfer in ref. 14). Essentially, three criteria are required: one for determining when transition precludes separation; a second for determining when the detached flow will not reattach to the surface and form a bubble; and a third for evaluating the extent of the bubble when it is formed. Of these three, only the latter two have been considered in any detail and, as yet, no completely satisfactory criteria have been found. The suggested criteria are either inconclusive due to the lack of experimental data or inconsistent with results from subsequent experiments.

It was the purpose of the present investigation to obtain measurements which would define a large number of regions of separated flow for a wide range of Reynolds numbers and pressure gradients. It was anticipated that in this manner, the existing physical interpretations of the flow in a bubble could be checked in greater detail than in the past and, at the same time, it was hoped that the data would provide further insight into the conditions which determine the occurrence and extent of laminar-separation bubbles.

NOTATION

The symbols used throughout this report are defined as follows:

c	airfoil chord, ft
H	total pressure, lb/sq ft
L	length of separated laminar flow, measured along surface, ft
p	static pressure, lb/sq ft
R	Reynolds number, $\frac{U_o c}{\nu}$
$R_{\delta_{sep}}$	Reynolds number, $\frac{U_{sep}\delta_{sep}}{\nu}$
R_L	Reynolds number, $\frac{U_{sep}L}{\nu}$

R_{s_l} Reynolds number, $\frac{U_o s_l}{\nu}$

$R_{s_{l_{sep}}}$ Reynolds number, $\frac{U_{sep} s_l}{\nu}$

R_λ Reynolds number, $\frac{U_{sep} \lambda}{\nu}$

s distance along upper surface, measured from the leading edge, ft

S pressure coefficient, $\frac{H_o - p}{H_o - p_o}$

u velocity inside the boundary layer, ft/sec

U velocity outside the boundary layer, ft/sec

x distance along airfoil chord line, measured from the leading edge, ft

y distance above surface, measured normal to the surface, ft

α geometric angle of attack, deg

s_l distance along surface from stagnation to separation, ft

s_p distance along surface from minimum pressure to separation, ft

σ $\frac{s_p}{s_l}$, dimensionless

δ boundary-layer thickness, arbitrarily defined as the distance above the surface where $u/U = 0.707$, ft

δ^t total boundary-layer thickness, ft

δ^* boundary-layer displacement thickness, $\int_o^{\delta^t} \left(1 - \frac{u}{U}\right) dy$, ft

η $\frac{y}{c}\sqrt{R}$

ρ mass density, slugs/cu ft

ν kinematic viscosity, sq ft/sec

λ total length of separated flow, measured along the surface, ft

Subscripts

sep position of laminar separation

o free stream

APPARATUS AND METHODS

Models

Two 5-foot-chord models were employed for this investigation. One was contoured to the coordinates of the NACA 663-018 airfoil section and the other to a symmetrical airfoil section having a thickness ratio of approximately 10.5 percent of the chord (table I). For simplicity, the thinner airfoil will hereinafter be referred to as the NACA 0010 (modified) airfoil. The models, constructed of laminated pine with a veneer of 1/8-inch-thick mahogany plywood, spanned the 7-foot dimension of one of the Ames 7- by 10-foot wind tunnels to simulate two-dimensional flow. Circular end plates, 6 feet in diameter, were attached to the models and formed part of the wind-tunnel floor and ceiling. The surfaces of the models were finished with lacquer and sandpapered and waxed to a high gloss. Flush pressure orifices (as noted in table II) were provided along the midspan of each model. A photograph of the NACA 663-018 airfoil installed in the wind tunnel is presented in figure 1.

Equipment

Boundary-layer surveys were made using the apparatus shown in figure 2. The apparatus, remotely controlled from outside the wind tunnel, consisted of three basic components: base, screw, and lever assemblies. The base is hollow and is provided with a small O ring which acts as a pneumatic seal. By venting the interior of the base to a vacuum pump, sufficient suction is obtained to make the apparatus adhere to the surface. Rotation of the screw assembly rotates the lever about its fulcrum and adjusts the ends of the survey tubes to the desired distance above the surface with an accuracy of ±0.0005 inch. The distance above the surface was measured with a micrometer microscope and was calibrated at each chordwise station against a dial reading in the control unit.

The probe was constructed of stainless-steel tubing and consisted of two total-pressure and one static-pressure tube. For rigidity, 0.0625-inch-outside-diameter tubing was employed where the probe joined the lever, and successively smaller diameters were then sleeved into the main support. At the plane of survey, 7.5 inches upstream of the base, 0.015- or 0.020-inch-outside-diameter tubing was used, depending on the thickness of the boundary layer to be measured. The ends of the total-pressure tubes were flattened to approximately oval shape and the wall thickness was reduced by honing with fine emery paper. All distances

above the surface were measured to the center line of the tube opening. The end of the static-pressure tube was constructed from 0.030-inch-outside-diameter tubing. Four static-pressure orifices, 0.008-inch diameter, were provided.

The hot-wire anemometer employed for observing the velocity fluctuations in the boundary layer and for measuring the free-stream turbulence was designed to operate the heated wire at a constant temperature. The amplifier had a flat response from 10 cycles to 180 kilocycles per second, but for the present investigation filters were incorporated which limited the response to less than 12 kilocycles per second. A special circuit was provided to compensate for heat lag in the wire. The square-wave technique described by Kovasznay in reference 15 was used to determine the proper compensation. Tungsten wire, nominally 0.00015-inch diameter, was spot welded to the ends of common sewing needles for the hot-wire probe; the wire length was approximately 0.1 inch (fig. 3). The probe was attached to the models with a vacuum base similar to that described previously. The sensitivity of the equipment was adjusted so that only fluctuations (root-mean-square values) greater than about 0.07 percent of the mean flow were measured.

For investigating the effects of turbulence, the turbulence level of the wind tunnel was increased by the installation of a net woven from commercial hard-drawn seine twine. The twine had a nominal diameter of 5/32 inch and the mesh of the net was 2.5 inches square. The net was positioned 40 mesh lengths upstream of the leading edges of the models.

All pressures were measured using liquid-in-glass, multiple-tube manometers. For the pressure distributions along the surface of the models, vertical manometers with either water or tetrabromoethane (specific gravity approximately 1.96) were employed. The boundary-layer surveys were obtained using an inclined alcohol manometer.

Test Conditions

All data were obtained for constant values of the Reynolds number, R, equal to 1.5, 2, 3, 4, 6, 8, and 10 million. The corresponding range of the free-stream Mach number and dynamic pressure was approximately 0.04 to 0.29 and 2.5 to 120 pounds per square foot, respectively. Throughout this range of variables the turbulence (streamwise component) of the wind-tunnel air stream without the net was 0.15 to 0.20 percent of the free-stream velocity. This level of turbulence occurred in a small core, approximately 18 inches in diameter, around the longitudinal center line of the wind tunnel. From this core the turbulence gradually increased to approximately 0.5 percent, 12 inches from the wind-tunnel walls. Since all measurements of the separated flow were taken at the midspan of the models, the minimum value of turbulence is representative for all data presented herein except when the turbulence net was installed. Installation of the net increased the turbulence to approximately 1.1 percent

across the midspan of the models. All data presented herein, except where noted, correspond to the turbulence level of the wind tunnel without the net.

Test Procedures

The pressure distributions, for 1° increments of angle of attack, were determined first for each airfoil in order to provide an indication of the approximate locations of the regions of separated flow. For Reynolds numbers of 8 and 10 million, high angles of attack were not investigated due to limitations of the manometers.

With the approximate locations of the separated flows known, measurements were made to ascertain the positions of laminar separation, transition, and flow reattachment so that the extents of separated laminar flow and the total extents of separated flow could be defined. Positions of laminar separation near the leading edges of the airfoils were ascertained by the liquid-film method described in references 6 and 16. Although, in several instances, spanwise variations in the position of separation were as large as 0.10 inch, all determinations of the position of separation were made at the same spanwise station as the pressure orifices and were measured to the nearest 0.01 inch. No measurements of this type were attempted for Reynolds numbers greater than 6 million because of the excessive time required to start and stop the wind tunnel. For the lowest Reynolds numbers and angles of attack, the liquid-film method did not give a satisfactory indication of separation due to insufficient shearing forces in the boundary-layer flow; for this reason the positions of separation near midchord on the NACA 663-018 airfoil were determined from detailed boundary-layer surveys.

The positions of transition from laminar to turbulent flow in the regions of separated flow were ascertained primarily from the pressure distributions by the method outlined in Appendix A. Hot-wire anemometer observations were also employed in some instances to verify the positions of transition indicated by the pressure distributions.

Positions of flow reattachment as indicated by the liquid-film technique (ref. 6) were vague and, consequently, near the leading edges they were ascertained instead by indications of a single total-pressure tube on the surfaces of the models. Reattachment at a given chordwise station was determined within a range of 0.5° angle of attack. Positions of flow reattachment were ascertained near midchord on the NACA 663-018 airfoil only for a Reynolds number of 2 million and angles of attack of 0° and 2°.

Preliminary studies revealed that use of the boundary-layer survey probe should be limited, due to probe deflections, to local dynamic pressures at the vacuum disk less than approximately 30 pounds per square foot. As a result, boundary-layer surveys were conducted only for a Reynolds

number of 2 million. All surveys were conducted at the same spanwise station as those of the flush pressure orifices in the models. Detailed surveys of the boundary-layer flow through the regions of separated flow were made only near midchord on the NACA 663-018 airfoil for angles of attack of 0° and 2°. These data were obtained to ascertain the positions of laminar separation and to afford a comparison with the data of Bursnall and Loftin in reference 8. Boundary-layer surveys near the leading edges of both airfoils were restricted to determining the boundary-layer thickness at separation δ_{sep}.

Investigation of the effects of increased free-stream turbulence was confined to pressure distribution and hot-wire-anemometer observations.

RESULTS AND DISCUSSION

Pressure Distributions

Pressure distributions along the surface on the NACA 0010 (modified) and 66_3-018 airfoils are presented in figures 4 and 5, respectively.[1] Due to the bulk of the pressure data, only typical distributions are shown to illustrate the effect of Reynolds number for several angles of attack. The highest values of angle of attack presented (12° and 15°, respectively, for the 10.5- and 18-percent-thick airfoils) correspond approximately to conditions for maximum lift. For higher angles of attack, depending on the Reynolds number, the airfoils either stalled or the flow became unsteady so that duplication of conditions for a series of measurements was uncertain. The stalls of both airfoils were abrupt for values of Reynolds number less than 6 million and were accompanied by a complete collapse of the leading-edge pressure peaks. This type of stall is apparently the result of a complete flow separation near the leading edge caused by separation of the laminar boundary layer without subsequent flow reattachment (e.g., ref. 10). The stalls, however, became more gradual as the Reynolds number was increased to values greater than 4 million. The change in stalling characteristics is significant since it indicates that between Reynolds numbers of 4 and 6 million the regions of separated flow near the leading edges experienced a change in conditions which prevented (or at least delayed) a complete flow separation following the occurrence of laminar separation.

It will be noted that, in general, the pressure distributions are faired to indicate abrupt breaks in the curves. As is shown in Appendix A, the positions of these breaks correspond to the positions at which transition from laminar to turbulent flow was completed. The poor definition of

[1]Data are presented herein as a function of the distance along the surface s rather than chordwise distance x. The relationship between the two measures of distance is tabulated in table II as determined by measurements of the two models.

the distributions for the lowest Reynolds number is attributable to the smallness of the manometer deflections.

Measurements Near the Leading Edges of the Airfoils

Position of laminar separation.- The positions of laminar boundary-layer separation $(s/c)_{sep}$ near the leading edges of the two airfoils (as determined by the liquid-film technique) are presented in figure 6. No separated flow was observed by this method for angles of attack less than 4° and 7° for the 10.5- and 18-percent-thick airfoils, respectively. Data for angles of attack greater than 12° and 15°, respectively, were not obtained because of the imminence of the stall.

Within the limitations of these measurements, the position of laminar separation for a given angle of attack was independent of the Reynolds number for Reynolds numbers from 1.5 million to 6 million. For a given pressure distribution this result, of course, would be expected, but since the pressure distributions for a given angle of attack (see figs. 4 and 5) varied with Reynolds number,[2] some change in the position of separation with Reynolds number (fig. 6) might be anticipated. The apparent variations in the pressure distributions are, however, primarily changes in the absolute magnitude of the coefficients rather than modifications of the distributions. As a result, any changes in the positions of separation with Reynolds number were negligibly small, and it is assumed in subsequent analyses that the positions of laminar separation for Reynolds numbers of 8 and 10 million are the same as for the lower values of Reynolds number.

It is interesting to note in connection with figures 4 and 5 that the occurrence of laminar separation and the presence of locally separated flow was not always accompanied by a region of essentially constant pressure. Regions of constant pressure observed in previous investigations are not apparent in figures 4 and 5 except for the lowest values of Reynolds number.

Boundary-layer thickness at position of laminar separation.- The variation of the boundary-layer thickness at separation $(\delta/c)_{sep}$ with angle of attack is presented in figure 7 for conditions near the leading edges of the two airfoils. These data were obtained for a Reynolds number of 2 million by boundary-layer surveys at the positions of separation (faired curves) shown in figure 6. The determination of δ_{sep} for higher values of Reynolds numbers was, as mentioned previously, precluded by limitations in the survey probes. However, in order to provide values of δ_{sep} throughout the Reynolds number range from 1.5 to 10 million, it is assumed that δ_{sep}/s_l varied in proportion to $\frac{1}{(U_{sep}/U_o)\sqrt{R_{s_l}}}$. This

[2]Due in part to associated changes in Mach number.

assumption follows directly from the analysis in reference 17 which indicates that the ratio $R_{\delta_{sep}}/\sqrt{R_{s_l}}$ is constant for a prescribed pressure distribution. The term U_{sep}/U_o is a correction factor to allow for the change which occurred in the magnitude of the pressure coefficient with Reynolds number for a given angle of attack. The correction was generally less than 8 percent and never exceeded 11 percent for the results presented herein.

Position of transition to turbulent flow.- Figure 8 presents the variation of the position of transition with angle of attack as determined by the method discussed in Appendix A for the two airfoils for all values of the Reynolds numbers investigated. The curves represent the faired values employed in subsequent analyses. The position of laminar separation has been included in figure 8 to show the large variation in the extent of separated laminar flow with Reynolds number. With the thinner airfoil for a Reynolds number of 10 million, transition is indicated to have occurred upstream of the position for laminar separation for an angle of attack of 4°. A similar result is also shown for the NACA 663-018 airfoil for all values of Reynolds number for 6° angle of attack.

Position of reattachment of the turbulent flow.- The positions of flow reattachment measured on the two airfoils are presented in figure 9. These data are limited to the same angles of attack and Reynolds numbers for which the liquid-film technique was employed. The positions of laminar separation from figure 6 are included to indicate the total extent of the regions of separated flow. When these results are compared with those in figure 8, it is interesting to note that the length of separated laminar flow L was about 75 to 85 percent of the total extent of separated flow λ.

Comparison of experimental and calculated positions of laminar separation.- In order to provide some basis for analyzing the conditions under which transition precluded laminar separation and the formation of a bubble, positions of laminar separation were calculated for such conditions for both the NACA 0010 (modified) and 663-018 airfoils after the tests were completed. These calculations were first performed for angles of attack for which a bubble was known to have formed to provide a comparison between experimental and calculated positions of laminar separation. Results of these first calculations for conditions near the leading edges of the airfoils are summarized in the following paragraph. The calculated positions of laminar separation near midchord on the NACA 663-018 airfoil and for conditions when transition precluded the formation of a bubble are discussed in subsequent sections. The method of Wieghardt was employed for the calculations (ref. 18).

It was found that positions of laminar separation calculated by the method of reference 18 were in good agreement with the positions measured experimentally for conditions near the leading edges of the two airfoils when a bubble did occur. For example, on the NACA 0010 (modified) airfoil

for an angle of attack of 4°, the calculated[3] and experimental positions of separation differ by slightly less than 4 percent of the total extent of laminar boundary-layer flow (values of $(s/c)_{sep}$ equal to 0.0381 and 0.0395, respectively). For the NACA 663-018 airfoil at an angle of attack of 7°, the calculated and experimental results differ by less than 1 percent of the total extent of laminar boundary-layer flow (values of $(s/c)_{sep}$ equal to 0.0280 and 0.0283, respectively). It should be mentioned that the calculated boundary-layer thicknesses at the positions of separation $(\delta/c)_{sep}$ for these two conditions are 2.5×10^{-4} and 2.0×10^{-4} for the NACA 0010 (modified) and 663-018 airfoils, respectively; the corresponding values estimated from measurements at Reynolds numbers of 2 million are, respectively, 2.45×10^{-4} and 1.65×10^{-4}. No explanation can be given for the large (approximately 17 percent) discrepancy between the two values for the thicker airfoil, particularly in view of the excellent agreement obtained for the NACA 0010 (modified) airfoil.

Measurements Near the Midchord of the NACA 663-018 Airfoil

Boundary-layer surveys.- The results of boundary-layer surveys for a Reynolds number of 2 million near the midchord of the NACA 663-018 airfoil are presented in terms of the velocity profiles through the regions of separated flow in figure 10 for angles of attack of 0° and 2°, respectively. No separated flow was observed for angles of attack greater than 2°. Thus, for the NACA 663-018 airfoil, transition apparently precluded separation for angles of attack from 3° to 6° inclusive.

The bubble shapes (the regions bounded by the airfoil surface and the contour along which the measured value of $u/U = 0$) derived from the velocity profiles are presented in figure 11. The upstream edges of the bubbles, which should correspond to the positions of laminar separation, indicate that separation occurred at values of s/c equal to approximately 0.62 and 0.61 for angles of attack of 0° and 2°, respectively. These indicated positions of laminar separation, however, are suspect and the validity of the measurements will be considered in a subsequent discussion.

Position of transition to turbulent flow.- The positions of transitions near midchord on the NACA 663-018 airfoil are shown in figure 8(b) for Reynolds numbers from 1.5 to 10 million. Since the pressure orifices in this region were more widely spaced than the orifices near the leading edge, all indications of transition in the pressure diagrams were checked throughout the Reynolds number range by means of hot-wire anemometer observations.

Comparison with results from reference 8.- Similar measurements in the region of separated flow near midchord on the NACA 663-018 airfoil are

[3]All calculations were based on the pressure distributions measured for a Reynolds number of 4 million.

presented by Bursnall and Loftin in reference 8 for 0° angle of attack and Reynolds numbers of 1.2, 1.7, and 2.4 million. Although a direct comparison cannot be made for a specific value of Reynolds number, the data from reference 8 together with data from the current investigation afford a comparison of results obtained in different wind-tunnel facilities with somewhat different experimental techniques. A detailed comparison is not warranted, however, in view of the uncertainty in the measured positions of laminar separation discussed in the following section.

Figure 12 presents a comparison of the shape and position of the bubbles. Although the indicated positions of separation are different for the two investigations, good correlation is obtained both as to the shape and the extent of the bubbles.

Positions of transition to fully turbulent flow from the two investigations are compared in the following table:

$R \times 10^{-6}$	s/c for transition	Source
1.2	0.745	Ref. 8
1.7	.725	Ref. 8
2.0	.715	Present investigation
2.4	.704	Ref. 8
3.0	.705	Present investigation
4.0	.690	Present investigation

The results correlate even though the turbulence level of the air stream for the reference data is a few hundredths of 1 percent in contrast to 0.15 to 0.20 percent for the current investigation.

Comparison of experimental and calculated positions of laminar separation.- As mentioned previously, positions for laminar separation were calculated to provide a comparison with measured positions of separation prior to analyzing conditions under which transition precluded the formation of a bubble. These calculations included conditions on the NACA 663-018 airfoil for angles of attack of 0° and 2°.

Due to the scatter in the pressure-distribution data for Reynolds numbers less than 3 million, it is not possible to calculate the boundary-layer flow for the same Reynolds number (2 million) for which the detailed boundary-layer surveys were obtained. Consequently, the calculations were performed employing the pressure distributions measured for a Reynolds number of 4 million. Separation was determined to have occurred at s/c equal to approximately 0.66 in contrast to 0.62 and 0.61 indicated by the boundary-layer surveys for 0° and 2°, respectively. The difference between the calculated and experimental positions of separation represents over 40 percent of the measured extent of separated laminar flow for a

Reynolds number of 2 million and the calculations indicate that transition precluded separation for Reynolds numbers greater than approximately 8 million.

There is some evidence in reference 8 and figure 5(a) that the position of minimum pressure moves upstream as the Reynolds number is reduced to less than 3 million. This, of course, would tend to move the calculated position of separation upstream and into better agreement with the positions of separation determined experimentally. Such an effect of Reynolds number on the position of separation, however, appears to be small. By use of data from reference 8 for Reynolds numbers of 1.2 and 2.4 million, positions for separation were calculated at values of s/c between the limits of 0.645 to 0.66 and 0.65 to 0.66, respectively, depending on the manner in which the pressure data are faired. Separation was measured at a value of s/c equal to approximately 0.635. A comparison of the pressure distributions from these tests and reference 8 for Reynolds numbers of 4 and 2.4 million, respectively, is presented in figure 13.[4]

In view of the author's experience with the method of calculation employed herein, the magnitude of the discrepancies between calculated and experimental results is considered significant and casts doubt on the validity of the experimental results. In this connection it is interesting that for values of s/c from 0.61 to 0.65 the shape, thickness, and growth of calculated velocity profiles are in good agreement with the experimental profiles except in the immediate vicinity of the surface. This result suggests that limitations in the probe and its attendant interference were the principal factors which influenced the measurements. Accordingly it is emphasized that data for conditions near midchord on the NACA 663-018 airfoil presented herein and in reference 8 should be used with caution. This reservation applies only to the boundary-layer surveys but, for this reason, these data are not employed in subsequent analyses.

Effects of Increased Turbulence on the Position of Transition

The effect of an increase in the free-stream turbulence on the position of transition in the regions of separated flow was examined briefly on the NACA 663-018 airfoil. As would be expected, the increased turbulence due to the turbulence net moved the transition upstream for all conditions.

---

[4]The results from reference 8 have been normalized so that the values of the pressure coefficient S at the position of minimum pressure are equal for both investigations. This procedure affects only the magnitude of the coefficients and does not affect the calculated position of separation.

For angles of attack of 0° and 2°, the bubble near the midchord was eliminated for a Reynolds number of 1.5 million. The exact position of transition was not determined, but it is known that it occurred upstream of the 50-percent-chord station. No bubble occurred, of course, for the higher values of Reynolds number.

In contrast, the regions of separated flow near the leading edge were not eliminated but were considerably reduced in extent compared with those without the turbulence net. The positions of transition near the leading edge with the net are shown in figure 14. The positions of separation included in the figure are the same as in figure 6. Although no liquid-film measurements were made with the net installed, pressure diagrams indicated that little change in the positions of separation accompanied the increase in turbulence level; that is, the net caused little change in the pressure distributions except for the indication of earlier transition. The upstream movement of transition implies a similar displacement in the position of flow reattachment. It is interesting to note that the increased level of turbulence reduced the extent of separated laminar flow near the leading edge in almost the same proportion as did a twofold increase in Reynolds number with the net removed. Thus, for example, an increase in Reynolds number from 2 to approximately 4 million with the net removed had almost the same effect on the extent of separated laminar flow as did an increase in turbulence level for a constant value of Reynolds number of 2 million. These results are a good example of an increase in free-stream turbulence raising the effective Reynolds number of the flow.

Analysis of Conditions Determining the Occurrence and Extent of Laminar-Separation Bubbles

In analyzing the conditions which determine the occurrence and extent of laminar-separation bubbles two basic questions are involved: (1) Under what conditions will a bubble be formed and (2) what is the extent of the bubble when one is formed? As mentioned in the INTRODUCTION, the formation of a bubble depends on two phenomena: The laminar boundary-layer flow must separate from the surface (transition must not preclude separation) and the detached flow following separation must reattach to the surface. It is convenient, however, for purposes of analysis to consider the first of these two phenomena which determines the occurrence of a bubble in terms of the extent of separated flow. In so doing, the conditions which cause transition to preclude separation and the formation of a bubble (a bubble of zero length) may be thought of as special conditions which arise from and are a part of the general conditions controlling the extent of separated flow. In the following sections, therefore, the discussion is divided into two parts. In the first, consideration is given to the conditions which determine whether or not flow reattachment will occur, while in the remainder of the discussion consideration is given to the extent of separated flow when a bubble is formed, including bubbles of zero extent.

Data from the current investigation are tabulated in table III in the form of nondimensional lengths and parameters employed during this and previous investigations. Due to the uncertainties in the positions of laminar separation, data for conditions near midchord on the NACA 663-018 airfoil are not presented. It is to be emphasized that the data are based on measurements of the boundary-layer thickness at separation δ_{sep} for a Reynolds number of 2 million. The values of δ_{sep} for other Reynolds numbers were computed by assuming that the boundary-layer thickness varied inversely with $(U_{sep}/U_o)\sqrt{R_{s_l}}$ for a given angle of attack.

Flow reattachment.- The first interpretation of the flow in regions of separated laminar flow was probably that made by von Doenhoff (ref. 3) on the basis of some measurements along a flat plate in a stream with an adverse pressure gradient. Considering the flow near an airfoil leading edge, von Doenhoff speculated that following laminar separation detached flow continues downstream along a path which is essentially a tangent to the surface at the position of separation (see accompanying sketch). At some point along this path transition takes place and the resultant expansion of the turbulent fluid effectively serves to deflect the inner boundary of the detached flow back toward the surface. The point at which this inner boundary of the detached flow touches the surface corresponds to the position of flow reattachment. Von Doenhoff assumed that $R_L = U_{sep}L/\nu$ can be taken as a constant, and suggested a value of 50,000 on the basis of his experimental results. With the spread of a turbulent jet as a criterion, the deflection angle θ was taken to be 15°. The extent of a region of separated flow is determined graphically, and the conditions under which flow reattachment will not occur are determined by the lengths of separated laminar flow for which the deflected flow after transition does not touch the surface.

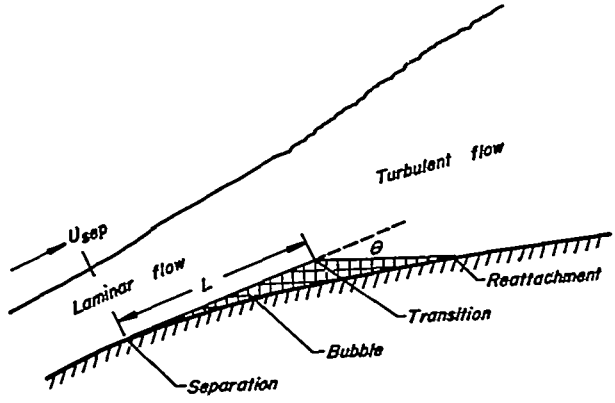

This simple picture of a region of separated flow has provided a good qualitative basis for explaining many of the effects of Reynolds number on the maximum lift and stalling characteristics of airfoil sections (e.g., refs. 10 and 19), and is remarkable in that it was developed with a minimum of experimental evidence. However, it was never intended to furnish a strict quantitative description of the flow processes involved.

To illustrate the limitations of this description of the bubble, the accompanying table presents values of the effective deflection angle θ ascertained from results of this investigation. The values were obtained graphically from the measured positions of separation, transition, and flow reattachment and the paths of separated laminar flow were approximated with lines tangent to the surface at the positions of separation.

NACA 0010 (Modified)					NACA 663-018		
α, deg	Effective deflection angle θ for R =			α, deg	Effective deflection angle θ for R =		
	2×10^6	4×10^6	6×10^6		2×10^6	3×10^6	6×10^6
4	(1)	15°	7°	7	52°	26°	6°
6	20°	34°	12°	9	40°	28°	15°
8	28°	26°	15°	11	32°	18°	23°
10	42°	21°	(2)	13	29°	26°	26°
13	31°	10°	(2)	15	45°	35°	28°

(1)Position of flow reattachment not measured.
(2)Bubble too small to determine value of θ.

At first appearance it would seem that no unique value of θ exists. It must be remembered, however, that these tabulated values of θ depend on the direction of the separated flow assumed between the positions of separation and transition. If the path of the detached flow deviated significantly from a line tangent to the surface at the position of separation, the values of θ listed in the table would be incorrect. Consequently, the current results are not sufficient proof to conclude that no unique value exists for an effective deflection angle. It is possible that the physical concept of an effective deflection angle having a constant value is essentially correct, in which case the tabulation may be interpreted to indicate that the path of the detached flow cannot be approximated by a line tangent to the surface at the position of separation. The primary cause for the disagreement between von Doenhoff's assumptions and the current results cannot be assessed with the available evidence. Nevertheless, it is apparent that the schematic representation of a bubble from reference 3 oversimplifies the process of flow reattachment in a laminar separation bubble. It is of interest to note that flow reattachment, as indicated by a line tangent to the surface at the position of separation, the experimental values of L, and a value of θ of 15°, would not occur on the NACA 663-018 airfoil at a Reynolds number of 2 million for any of the angles of attack shown in the table.

The occurrence of flow reattachment as given by the schematic representation of a bubble from reference 3 is, of course, also dependent on the extent of separated laminar flow L. The length L, however, appears to be closely related to the total extent of separated flow λ, and the validity of the assumption that R_L is a constant having a value of 50,000 is discussed later.

Since von Doenhoff's original speculations concerning the characteristics of a laminar separation bubble, only Maekawa and Atsumi (ref. 9) and Owen and Klanfer (ref. 14) are known to have suggested what the conditions are which determine whether or not separated flow will reattach once laminar separation does take place. Maekawa and Atsumi obtained

measurements of regions of separated flow downstream of the intersection of two plane surfaces. On the basis of these measurements they concluded that reverse flow in the bubble forms a vortex motion which attracts the detached flow toward the surface. Flow reattachment will not occur unless sufficient vorticity is supplied to maintain this vortex motion. As a measure of the vorticity required for the occurrence of reattachment, Maekawa and Atsumi suggested that the boundary-layer Reynolds number $R\delta^t_{sep}$ must be greater than a critical value of approximately 1200. They also suggested that if the Reynolds number based on the total extent of separated flow R_λ becomes too large, it is impossible to maintain the vortex against dissipation. As a result R_λ must be less than a certain critical value which they found depends on the turbulence level of the free stream. For a turbulence level about equal to that for the present investigation without the turbulence net installed, Maekawa and Atsumi found the critical value of R_λ to be 75,000. The first of these two conditions is essentially the same as a criterion proposed by Owen and Klanfer based on an analysis of available experimental data including some measurements obtained in supersonic flows. Owen and Klanfer suggest that reattachment will always occur when $R\delta^*_{sep}$ is greater than approximately 400 to 500.

Before these criteria are compared with the results from the current investigation, it is necessary to point out the relationships between the parameters employed herein and in references 9 and 14. An approximate relationship between L and λ from the current results has already been mentioned (L is approximately 0.8 λ, at least for a bubble near the leading edge of an airfoil) so that the critical value of R_λ from reference 9 corresponds to approximately 60,000 in terms of R_L. For conditions at a position of laminar separation, the so-called exact solutions of the boundary-layer equations of motion for a wide range of pressure distributions (i.e., Hartree, ref. 20; Howarth, ref. 21; and Tani, ref. 22) indicate that the ratio $\delta_{sep}/\delta^*_{sep}$ is constant and equal to 1.25. The quantity δ^t for exact solutions is, of course, indefinite but if δ^t is defined as the distance above the surface for which u/U attains a value of 0.999, the ratio $\delta^t_{sep}/\delta_{sep}$ is approximately constant and equal to 2.0. With these ratios the critical value of the boundary-layer Reynolds number from reference 9 becomes 600 in terms of $R\delta_{sep}$ and, similarly, a range from 500 to 625 for the critical values suggested in reference 14. Note that the value from reference 9 is within the limits given by reference 14.

Consider first the concept of the existence of a critical value of the boundary-layer Reynolds number at separation for the occurrence of flow reattachment. Table III shows that for all the conditions in the current tests when a bubble was present, the values of $R\delta_{sep}$ exceeded the critical values suggested in references 9 and 14. To this extent, these data are consistent with the criteria in reference reports. Contrary to the criterion suggested by Owen and Klanfer, however, the results from this investigation show that the occurrence of flow reattachment

cannot be determined solely by the use of a unique or critical value of $R\delta_{sep}$. It is indicated in table III that different values of $R\delta_{sep}$ existed on both airfoils for different values of the test Reynolds numbers immediately prior to the abrupt stalls. These values varied from approximately 900 to 1900 and 650 to 1500 for the NACA 0010 (modified) and 663-018 airfoils, respectively. Moreover, since $R\delta_{sep}$ appears to have been very nearly independent of angle of attack for a given airfoil and test Reynolds number, the apparently critical values of $R\delta_{sep}$ were critical only for the angles of attack at which the airfoils stalled. This result, however, does not imply that the critical values of $R\delta_{sep}$ from references 9 and 14 are in error. It appears, as suggested by Maekawa and Atsumi, that a value of $R\delta_{sep}$ equal to approximately 600 represents a lower limit beyond which conditions for flow reattachment can never occur. A value greater than approximately 600 assures only that flow reattachment is possible. It would seem that additional conditions, perhaps similar to the second one suggested in reference 9, determine whether or not flow reattachment will occur. However, it is apparent that the results in table III do not corroborate the second criterion from reference 9. Values of R_L as large as 170,000 were measured at the low angles of attack which obviously correspond to conditions for which the separated flow did reattach to the surface. In addition, the trends of the data for a given angle of attack indicate that values of R_L from approximately 35,000 to 70,000 probably existed when flow reattachment failed to occur and precipitated the abrupt stalls of both airfoils.

Attempts to determine additional conditions for the occurrence of flow reattachment from the current results were unsuccessful. At the present time, therefore, the physical conditions which determine the occurrence of flow reattachment are, in part, unknown. It seems probable that the surface curvature in the region of separated flow has a significant effect on reattachment. In this respect it is speculated that the bubble thickness at the position of transition may be an important parameter. If one considers two regions of separated flow having identical surface conditions and values of $R\delta_{sep}$ and R_L, it seems reasonable that the flow having the thicker bubble at the position of transition would be the least apt to reattach to the surface. The schematic representation of a bubble by von Doenhoff is fundamentally a procedure which attempts to evaluate such an effect of bubble thickness. Since, however, the path of the separated laminar flow probably cannot be defined by a line tangent to the surface at the position of separation, any analysis of parameters involving the bubble thickness must be based either on extensive and detailed boundary-layer measurements or, perhaps, on treatment of the bubbles as surface distortions or bumps and estimation of the bubble thicknesses from the magnitudes of the perturbation velocities.

Extent of separated flow.- The extent of separated flow in a bubble may be considered to consist of two distinct parts in a manner similar to that described in reference 3. The first and larger part of the bubble,

of course, is the extent of separated laminar flow while the remainder consists of a short region along which the separated turbulent flow returns to the surface to form a turbulent boundary layer. The current results indicate, as previously mentioned, that at least near the leading edge of an airfoil the length of separated laminar flow L is equal to an approximately constant percentage of the total extent of separated flow λ. This result suggests that there is little to choose from between either L or λ as a suitable reference length for describing the extent of a bubble for arbitrary conditions. The use of L, however, seems preferable in view of the fact that the variables which affect the extent of laminar flow (pressure distribution, surface roughness, free-stream turbulence, etc.) are known, at least qualitatively, while the variables which control the occurrence of flow reattachment are, essentially, unknown. Accordingly, in the remaining discussion only the length of separated laminar flow L is considered. The present results suggest that the total extent of separated flow may be taken equal to approximately 1.25 L.

In reference 3 von Doenhoff, as discussed in the previous section, speculated that the Reynolds number R_L was essentially a constant and equal to 50,000. Examination of table III reveals that this is a fair approximation for an average value of R_L for all the measurements from the present investigation. Nevertheless, it is apparent that no one value of R_L can be considered a universal constant. The use of a constant value of R_L, moreover, is not a realistic approach from physical considerations since it implies that transition can never preclude laminar separation.

Maekawa and Atsumi (ref. 9) also concluded that the term R_L was a constant and instead suggested a value of 25,000 based on their measurements. Although this result seemingly confirms von Doenhoff's original speculation that R_L has a constant value, there is considerable basis for questioning this result for the measurements reported in reference 9. For the investigation discussed in reference 9, neither the position of transition nor the direction of the separated flow downstream of the intersection of the two plane surfaces was measured. In order to ascertain values of L, therefore, Maekawa and Atsumi assumed different straight-line paths for the separated laminar flow and then selected the paths which gave a constant value for R_L in agreement with von Doenhoff's schematic representation of a bubble. In view of the previous comparisons with von Doenhoff's representation of a bubble, it is apparent that the basis for this method of analysis is invalid and that the values of R_L in reference 9 are probably in error. Further evidence of the uncertainty of the correctness of the values of R_L presented in reference 9 is the conclusion of Maekawa and Atsumi that free-stream turbulence up to a value of 1.7 percent does not affect the value of R_L. Such a conclusion is not corroborated by the current results (compare tables III and IV for the NACA 66_3-018 airfoil).

The fact that R_L is not constant should not be surprising. By assuming R_L to be constant, one also assumes, for all practical purposes, that L is dependent only on the velocity outside the boundary layer at the position of separation U_{sep}. Such an assumption is obviously oversimplified. However, it is surprising that over 80 percent of the values of R_L from the present investigation are within a range from 25,000 to 75,000, including most of the measurements obtained with the turbulence net installed. To examine this result further, consider that

$$R_L = \frac{U_{sep}L}{\nu} = \left(\frac{L}{s_l}\right)\left(\frac{U_{sep}s_l}{\nu}\right) = \frac{L}{s_l} R_{s_l sep}$$

so that for a given value of R_L

$$\frac{L}{s_l} \sim \frac{1}{R_{s_l sep}}$$

The distance s_l, introduced as a reference length representative of the laminar flow, is the extent of laminar boundary-layer flow between the positions of stagnation and separation. Of course any other reference length could be used to make the quantities dimensionless but s_l should be useful in the comparison of these results with those of other investigations. If R_L is essentially constant, L/s_l should form a unique correlation with $R_{s_l sep}$. The current results are presented in this manner in figure 15 and it is apparent that the bulk of the data are within the limits of values for R_L from 25,000 to 75,000. These results serve to illustrate that U_{sep} or, more correctly, some measure of the local Reynolds number is a prime variable controlling the extent of separated laminar flow L. Fundamentally, therefore, the use of a constant value of R_L is a first-order approximation for defining an extent of L for arbitrary conditions.

It is interesting to note that if, for a given pressure distribution, δ_{sep}/s_l is inversely proportional to $(U_{sep}/U_o)\sqrt{R_{s_l}}$, it is possible to express constant R_L by

$$R_{s_l sep} \sim \sqrt{R_{s_l}}\left(\frac{s_l}{\delta_{sep}}\right) \quad \text{and} \quad \frac{L}{s_l} \sim \left(\frac{\delta_{sep}}{s_l}\right)\frac{1}{\sqrt{R_{s_l}}}$$

Thus, the correlation shown in figure 15 and von Doehnoff's original speculation may be interpreted to mean that, for a given pressure distribution, an extent of separated laminar flow depends both on some measure of a local Reynolds number and on the boundary-layer thickness at the

position of separation. Since, for a given Reynolds number, δ_{sep} is known to be a function of the pressure distribution, this would indicate that L depends on the pressure distribution.

Essentially the same approach as that demonstrated in figure 15 is suggested by Bursnall and Loftin (ref. 8) for correlating the extent of separated laminar flows. They introduce the boundary-layer thickness at the position of separation δ_{sep} as a reference length (instead of s_l) and concluded that the ratio L/δ_{sep} was a function of the boundary-layer Reynolds number at separation $R_{\delta_{sep}}$. They found that their data together with the measurements from references 5 and 6 formed two fairly distinct correlations - one for conditions near the leading edge of an airfoil, and a second for conditions near the midchord of an airfoil. Since the measurements near midchord on the NACA 663-018 airfoil are suspect, the distinction between these two correlations may not be significant. The trends of both correlations, however, indicated there probably were critical values of $R_{\delta_{sep}}$ for which transition would preclude separation (i.e., as $R_{\delta_{sep}}$ increased, L/δ_{sep} decreased). The difference between the two correlations was attributed to differences in the pressure gradients and in the history of the flow preceding separation for the two conditions.

The correlation presented in the reference report is reproduced in figure 16 together with results from the current investigation for the two values of turbulence. The bulk of the data from this investigation conform with the groupings originally defined by Bursnall and Loftin, but it is apparent that, as for the correlation based on the reference length s_l (fig. 15), there is no simple relationship between L/δ_{sep} and R/δ_{sep}.

It became evident while comparing the results from this and previous investigations that the absolute magnitudes of L and δ_{sep} were interrelated. In this manner it was discovered that when L/s_l is considered to be a function of δ_{sep}/s_l for the data from the present investigation for the lower level of free-stream turbulence, a gross correlation is apparent for all the conditions near the leading edges of the two airfoils (fig. 17). Results from reference 6 appear to be consistent with the trend of this correlation which, for simplicity, can be expressed by an equation for a straight line.

$$\frac{L}{s_l} = d_1 + d_2\left(\frac{\delta_{sep}}{s_l}\right)$$

Attempts to refine this relationship by considering d_1 and d_2 as functions of different measures of pressure gradients were unsuccessful, but some dependence of L/s_l on the term σ is shown in figure 17. The term σ (where $\sigma = s_p/s_l$ and s_p is the distance between positions of minimum pressure and separation and s_l is, as defined before, the distance between the positions of stagnation and separation) should be

considered an approximate description of the pressure distribution along the surface upstream of separation for flow around the leading edge of an airfoil at moderate to high angles of attack. The trend of the correlation shown in figure 17 suggests the simple algebraic relationships

$$d_1 = -\frac{P_1}{P_2 - \sigma^m} \quad \text{and} \quad d_2 = P_3 + P_4\sigma^n$$

where, in view of the lack of complete correlation, the exponemts m and n and the quantities P_i (always positive valued) may depend on some additional measures of the pressure distribution. No further correlation, however, was found, but it appears that the terms m, n, and P_1 are essentially constants. Since the range of σ in the correlation is limited almost exclusively to values less than 0.3, a numerical evaluation of these terms as constants is not warranted at the present time.

In view of this apparent correlation between L/s_l, δ_{sep}/s_l, and σ presented in figure 17, one might expect that consideration of the parameter σ would permit some further refinement in the correlation between L/s_l and $R_{s_l}{}_{sep}$ shown in figure 15. Analysis of the data, however, reveals no simple functional relationship between L/s_l, $R_{s_l}{}_{sep}$, and σ.

Although the relationships for L, d_1, and d_2 are empirical and have no physical basis for their formulation, the correlation shown in figure 17 is significant because it provides an indication that the extent of separated laminar flow along a bubble depends in part on the pressure distribution. In this regard, the current results show that as σ increases the quantities d_1, and d_2 also increase; d_1 increases much more rapidly than d_2 and, as σ approaches a value of 1.0, d_1 probably tends to become negatively infinite while d_2 remains finite. Thus, an increase in σ tends to decrease an extent of separated laminar flow and approach conditions under which transition would preclude separation. For values of σ approaching 1.0, the existence of separated laminar flow would be virtually impossible except, perhaps, at exceedingly low values of Reynolds number.

The general applicability of the correlation and significance of σ for arbitrary conditions are difficult to ascertain without recourse to additional experiments. However, some further insight toward this end is provided by the current data for conditions under which a bubble did not occur on the two airfoils. For the NACA 0010 (modified) airfoil for angles of attack from 0° to 3°, inclusive, the minimum pressure was near the leading edge while laminar separation, as calculated by the method of reference 18, would have occurred in the vicinity of midchord. The ratio of σ for these conditions was of the order of 0.9 which, according to the previous discussion, would tend to eliminate the occurrence of a bubble in agreement with the experimental results. In contrast, the positions of minimum pressure on the NACA 663-018 airfoil for angles of attack from 0° to 2°, inclusive, were well back along the chord. The value of σ

for these conditions was of the order of 0.1, a value which, consistent with with the trend of the correlation, permitted the formation of a bubble. It is uncertain, however, whether or not the extent of separated laminar flows L for these conditions would fit the correlation shown in figure 17 for conditions near the leading edges of airfoils. If the positions of separation ascertained experimentally are essentially correct, a single correlation would result which would be applicable to conditions near either the leading edge or midchord. Such a correlation would be significant since it would indicate that the mechanics of the flow in a bubble are not dependent on local conditions. If, however, the calculated positions of separation are more nearly correct, the values of L near midchord do not correlate with the measurements obtained near the leading edges.

For the thicker airfoil in the range of angles of attack from 3° to 6°, inclusive, the position of minimum pressure suddenly moved forward to a position just downstream of the leading edge. The calculated positions of laminar separation, however, remained near midchord up to an angle of attack of 5° and σ was of the order of 0.9; for 6° angle of attack, separation would have occurred nearer the leading edge and σ was probably of the order of 0.6. Thus, the experimental results for the NACA 66_3-018 airfoil in the intermediate range of angles of attack are also consistent with the general trend of the correlation shown in figure 17.

It is evident from the preceding discussion that at the present time, the physical conditions which control the extent of separated laminar flow along a bubble are not known completely. The current results, it is thought, indicate that the principal factors which determine an extent of separated laminar flow are some measure of the local Reynolds number of the laminar boundary-layer flow and the boundary-layer thickness at the position of laminar separation. The pressure distribution upstream of separation, as described by the parameter σ, also affects the length of separated laminar flow. There are, however, many ramifications involved and the correlations presented may only show the trends of existing data. Additional measurements of bubbles, particularly for conditions when σ is greater than 0.3, are required to verify these trends. It is to be emphasized, moreover, that these trends correspond to conditions for only one value of free-stream turbulence and an aerodynamically smooth surface.

CONCLUSIONS

Measurements have been presented from an experimental investigation of regions of separated flow caused by separation of the laminar boundary layer (laminar separation "bubbles"). The measurements, obtained near the leading edges of two airfoils for a wide range of angles of attack and Reynolds numbers, have been compared with similar results from previous investigations and lead to the following conclusions:

1. The physical conditions which determine whether or not a bubble will form after the occurrence of laminar separation are, as yet, unknown. In this regard, however, apparently a necessary condition for the occurrence of a bubble, although not a sufficient condition, is that the boundary-layer Reynolds number at the position of laminar separation must be greater than a certain critical value; this critical value, determined by previous investigators and consistent with current results, is of the order of 500, based on the boundary-layer displacement thickness.

2. The extent of separated laminar flow along a bubble is approximately 75 to 85 percent of the total extent of separated flow, at least for conditions near the leading edge of an airfoil.

3. The extent of separated laminar flow along a bubble is dependent primarily on both the boundary-layer thickness at the position of laminar separation and on some measure of the local Reynolds number of the laminar boundary-layer flow.

4. There appears to be some relationship between the extent of separated laminar flow and the pressure distribution as described by the ratio of the distance between the positions of minimum pressure and laminar separation to the distance between the positions of stagnation and laminar separation.

5. An increase in the free-stream turbulence reduces the extent of separated laminar flow in a manner somewhat analogous to an increase in the Reynolds number.

6. The position of transition to fully turbulent flow along a bubble can be ascertained with good accuracy from detailed surface pressure-distribution measurements.

Ames Aeronautical Laboratory
National Advisory Committee for Aeronautics
Moffett Field, Calif., June 6, 1955

APPENDIX A

DETERMINATION OF THE TRANSITION POINT FROM EXPERIMENTAL PRESSURE DISTRIBUTIONS

Most of the previous experimental investigations of the bubble have shown an abrupt pressure increase along the surface upstream of the point where flow reattachment was considered to have taken place. Because of the abruptness of the pressure rise, the pressure distribution can be faired with an abrupt break in the curve which, where sufficient data are available, appears to coincide with the position where transition was completed. If this apparent correlation is generally true, it appears to offer a remarkably simple means for determining the transition point.[1] Moreover, the position of transition could be determined without a probe and its attendant interference.

Accordingly, at the beginning of the experimental investigation, detailed measurements of pressure distributions were obtained over the leading edge of the NACA 0010 (modified) airfoil (fig. 4) and the position of the break in the faired curve was determined as indicated by the schematic diagram.

Fairing of the curves was, in some instances, arbitrary but in most cases a break could be either pinpointed or defined along a short extent of surface less than half the distance between adjacent pressure orifices. By plotting these positions or regions of the breaks as a function of angle of attack, it was found that a smooth curve could be drawn which was arbitrary within extremely narrow limits. The limits were generally within s/c equal to ±0.0005, although for the lower angles of attack and Reynolds numbers the break took place between more widely spaced orifices and the uncertainty was of the order of ±0.001.

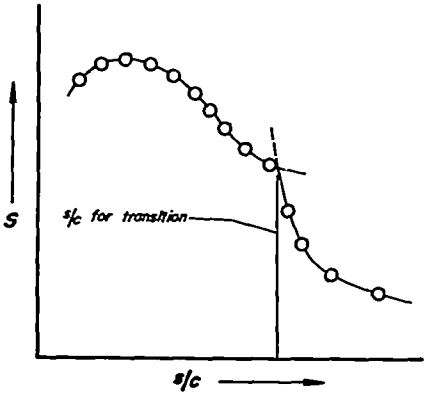

The positions of transition were then determined by use of the hot-wire anemometer. The hot-wire probe was placed at a given chordwise station and the angle of attack increased in 0.25° increments. For the lower angles of attack, the flow was steady. Gradual increases in angle of attack led to the intermittent appearance of completely random disturbances characteristic of turbulent flow. When completely turbulent

[1] Pfenninger (ref. 23) has used this method to determine the position of transition in regions where flow separation does not occur.

flow persisted, the angle of attack was noted and transition for that particular station was taken as having occurred midway in the final angle-of-attack increment.

The comparison between the breaks in the pressure diagrams and the hot-wire observations is shown in figure 18. Within the accuracy of the data, the two types of measurements give identical results. Since subsequent measurements revealed that the presence of the probe did not change the supposed position of transition indicated by the pressure distributions, it is concluded that the position of transition in a bubble may be determined easily and accurately from pressure-distribution diagrams. The positions of transition, therefore, were determined throughout the remainder of the investigation in this manner. In those cases where transition occurred between widely spaced pressure orifices, the pressure-distribution determinations were augmented with hot-wire observations for increased accuracy.

It is suggested that a second method, which would permit the use of fewer orifices, for determining the position of transition on an airfoil may be practicable. If the pressure coefficients for a given chordwise station (and Reynolds number) are plotted versus angle of attack, a break also occurs which coincides with the abrupt pressure increase accompanying the passing of transition over the orifice. A typical example of this second method is shown in figure 19. The angles of attack for which laminar separation and transition occurred at the static-pressure orifice are indicated on the figure as determined from figures 6 and 8, respectively. Finer increments in angle of attack would provide a better determination of the position of transition with this second method than that shown by the figure. It seems doubtful, however, if one method would be more accurate than the other.

REFERENCES

1. Jones, B. Melvill: An Experimental Study of the Stalling of Wings. R. & M. No. 1588, British A.R.C., 1934.

2. Jones, B. Melvill: Stalling. Jour. Royal Aero. Soc., vol. 38, no. 285, Sept. 1934, pp. 753-770. (22nd Wilbur Wright Memorial Lecture.)

3. von Doenhoff, Albert E.: A Preliminary Investigation of Boundary-Layer Transition Along a Flat Plate with Adverse Pressure Gradient. NACA TN 639, 1938.

4. Jacobs, Eastman N., and von Doenhoff, A. E.: Transition as It Occurs Associated with and Following Laminar Separation. Proc. Fifth Int. Congr. of App. Mech., 1938, pp. 311-314.

5. von Doenhoff, Albert E., and Tetervin, Neal: Investigation of the Variation of Lift Coefficient with Reynolds Number at a Moderate Angle of Attack on a Low-Drag Airfoil. NACA WR L-661, 1942.

6. Gault, Donald E.: Boundary-Layer and Stalling Characteristics of the NACA 63-009 Airfoil Section. NACA TN 1894, 1949.

7. McCullough, George B., and Gault, Donald E.: Boundary-Layer and Stalling Characteristics of the NACA 64A006 Airfoil Section. NACA TN 1923, 1949.

8. Bursnall, William J., and Loftin, Laurence K., Jr.: Experimental Investigation of Localized Regions of Laminar-Boundary-Layer Separation. NACA TN 2338, 1951.

9. Maekawa, T., and Atsumi, S.: Transition Caused by the Laminar Flow Separation. NACA TM 1352, 1952. (Translation of "Sōryu-Hakuri ni tomorrou Sen'i ni Kansuru Kenkyū," Jour. Soc. Appl. Mech. Japan, vol. 1, no. 6, Nov. 1949, pp. 187-192.)

10. McCullough, George B., and Gault, Donald E.: Examples of Three Representative Types of Airfoil Section Stall at Low Speed. NACA TN 2502, 1951.

11. Bursnall, William J., and Loftin, Laurence K., Jr.: Experimental Investigation of the Pressure Distribution About a Yawed Circular Cylinder in the Critical Reynolds Number Range. NACA TN 2463, 1951.

12. Delany, Noel K., and Sorensen, Norman E.: Low-Speed Drag of Cylinders of Various Shapes. NACA TN 3038, 1953.

13. Ackeret, J., Feldmann, F., and Rott, N.: Investigations of Compression Shocks and Boundary Layers in Gases Moving at High Speed. NACA TM 1113, 1947.

14. Owen, P. R., and Klanfer, L.: On the Laminar Boundary Layer Separation From the Leading Edge of a Thin Airfoil. Aero. Rep. 2508, British, R.A.E., Oct. 1953.

15. Kovasznay, Laszlo: Calibration and Measurement in Turbulence Research by the Hot-Wire Method. NACA TM 1130, 1947.

16. McCullough, George B., and Gault, Donald E.: An Experimental Investigation of the NACA 63_1-012 Airfoil Section with Leading-Edge Suction Slots. NACA TN 1683, 1948.

17. von Kármán, Th., and Millikan, C. B.: On the Theory of Laminar Boundary Layers Involving Separation. NACA Rep. 504, 1934.

18. von Wieghardt, K.: Über einen Energiesatz zur Berechnung laminarer Grenzschichten. Ingenieur-Archiv, XVI Bond #3-4, 1948, pp. 231-242. (A translation entitled "On an Energy Equation for the Calculation of Laminar Boundary Layers" has been published by the Joint Intelligence Objectives Agency, Washington, D. C.) Also available as ATI33090.

19. Loftin, Laurence K., and Bursnall, William J.: The Effects of Variations in Reynolds Number Between 3.0×10^6 and 25.0×10^6 Upon the Aerodynamic Characteristics of a Number of NACA 6-Series Airfoil Sections. NACA TN 1773, 1948.

20. Hartree, D. R.: On an Equation Occurring in Falkner and Skan's Approximate Treatment of the Equations of the Boundary Layer. Proc. Cambridge Phil. Soc., vol. 33, pt. 2, 1937, pp. 223-239.

21. Howarth, L.: On the Solution of the Laminar Boundary Layer Equations. Proc. Roy. Soc. of London, Ser. A, vol. 164, 1938, pp. 547-579.

22. Tani, Itiro: On the Solution of the Laminar Boundary Layer Equations. Jour. Phys. Soc. of Japan, vol. 4, no. 3, 1949, pp. 149-154.

23. Pfenninger, Werner: Investigations on Reductions of Friction on Wings, in Particular by Means of Boundary Layer Suction. NACA TM 1181, 1947.

TABLE I.- COORDINATES OF THE AIRFOIL SECTIONS

Station, percent chord	Airfoil section ordinate, percent chord	
	NACA 0010 (modified)	NACA 66_3-018
0	0	0
.5	1.08	1.323
.75	1.31	1.571
1.25	1.64	1.952
2.50	2.21	2.646
5.0	2.94	3.690
7.5	3.433	4.513
10.0	3.807	5.210
15	4.352	6.333
20	4.724	7.188
25	4.995	7.848
30	5.166	8.346
35	5.255	8.701
40	5.253	8.918
45	5.164	8.998
50	4.994	8.942
55	4.733	8.733
60	4.401	8.323
65	3.982	7.580
70	3.481	6.597
75	2.910	5.451
80	2.329	4.206
85	1.747	2.934
90	1.166	1.714
95	.583	.646
100	0	0
L.E. radius, percent chord:	1.304	1.955

TABLE II.- LOCATION OF PRESSURE ORIFICES

NACA 0010 (modified)			
Chordwise station x/c (nominal)	Distance along surface, s/c	Chordwise station x/c (nominal)	Distance along surface, s/c
0	0	0.075	0.087
.0020	.0035	.10	.112
.0025	.0070	.15	.163
.003[a]	.0076	.2	.213
.004	.0089	.25	.263
.005	.0098	.3	.313
.006[a]	.0113	.35	.363
.007	.0131	.4	.413
.008	.0144	.45	.463
.009	.0158	.5	.513
.010	.0171	.55	.563
.011[a]	.0183	.6	.613
.012	.0196	.65	.663
.013	.0208	.7	.714
.014[a]	.0220	.75	.764
.015	.0233	.8	.814
.016	.0242	.85	.865
.017	.0255	.9	.917
.018[a]	.0267	.95	.966
.020	.0287		
.022	.0310		
.024	.0330		
.026	.0352		
.028	.0373		
.030	.0393		
.032	.0414		
.034	.0435		
.036	.0455		
.038	.0477		
.042	.0517		
.045	.0569		
.05	.0622		
NACA 663-018			
0	0	0.100	0.119
.0007[a]	.0025	.15	.170
.001[a]	.0047	.2	.221
.002[a]	.0074	.3	.322
.003[a]	.0094 (.0097[a])	.4	.422
.004[a]	.0123 (.0119[a])	.5	.522
.005[a]	.0157 (.0145[a])	.55	.572
.006	.0168	.60	.622
.007	.0182	.61	.632
.008	.0194	.62	.643
.009	.0208	.63	.653
.010	.0222	.64	.663
.012[a]	.0247 (.0238[a])	.66	.683
.014	.0270	.68	.704
.016	.0294	.70	.724
.018	.0317	.72	.745
.020	.0339	.74	.765
.025[a]	.0394 (.0385[a])	.76	.786
.030	.0450	.78	.807
.035	.0504	.80	.827
.040	.0558	.85	.879
.045	.0610	.9	.930
.050	.0667	.95	.981
.075	.0920	.99	1.021

[a]Orifices on upper surface except at stations marked with a which were on both upper and lower surfaces.

TABLE III.- SUMMARY OF DATA FOR TURBULENCE LEVEL OF 0.15 TO 0.20 PERCENT (BASED ON THE ROOT-MEAN-SQUARE VALUE OF THE FLUCTUATING COMPONENT IN THE STREAMWISE DIRECTION)

(a) NACA 0010 (modified) Airfoil

R, million	α, deg	4	5	6	7	8	9	10	11	12
1.5	$L/c\times10^2$	7.33	2.55	2.00	1.60	1.37	1.26	1.20	1.11	1.06
	$^a(\delta/c)_{sep}\times10^4$	4.09	3.71	3.39	3.05	2.85	2.88	2.68	2.43	2.28
	$s_1/c\times10^2$	4.95	4.65	4.60	4.55	4.60	4.65	4.73	4.94	5.16
	U_{sep}/U_o	1.55	1.70	1.86	2.06	2.09	2.28	2.47	2.62	2.78
	$R\theta_{sep}$	950	930	930	880	890	920	940	910	920
	$R_L\times10^{-3}$	171.0	65.0	55.7	47.6	43.7	42.2	44.1	43.7	44.2
	s_p/s_1	0.452	0.310	0.226	0.220	0.217	0.237	0.240	0.210	0.182
2.0	$L/c\times10^2$	4.81	1.85	1.55	1.40	1.27	1.15	1.02	0.89	0.77
	$(\delta/c)_{sep}\times10^4$	3.50	3.08	2.83	2.50	2.33	2.25	2.08	1.92	1.83
	$s_1/c\times10^2$	4.95	4.65	4.60	4.55	4.60	4.65	4.73	4.94	5.16
	U_{sep}/U_o	1.57	1.77	1.92	2.11	2.29	2.48	2.69	2.88	2.96
	$R\theta_{sep}$	1100	1090	1090	1050	1050	1110	1120	1110	1110
	$R_L\times10^{-3}$	151.0	65.4	59.7	59.1	57.2	57.1	54.9	51.3	46.5
	s_p/s_1	0.452	0.310	0.226	0.220	0.217	0.237	0.240	0.210	0.182
3.0	$L/c\times10^2$	1.85	1.45	1.23	1.10	1.00	0.83	0.74	0.60	0.48
	$^a(\delta/c)_{sep}\times10^4$	2.87	2.59	2.32	2.08	1.90	1.85	1.68	1.58	1.49
	$s_1/c\times10^2$	4.95	4.65	4.60	4.55	4.60	4.65	4.73	4.94	5.16
	U_{sep}/U_o	1.55	1.72	1.92	2.08	2.26	2.45	2.72	2.87	3.03
	$R\theta_{sep}$	1350	1320	1330	1280	1290	1360	1390	1350	1370
	$R_L\times10^{-3}$	86.7	74.8	85.3	68.6	67.7	62.5	60.2	51.5	43.7
	s_p/s_1	0.452	0.310	0.226	0.220	0.217	0.237	0.240	0.210	0.182
4.0	$L/c\times10^2$	0.95	1.05	1.05	0.91	0.77	0.64	0.53	0.43	0.36
	$^a(\delta/c)_{sep}\times10^4$	2.45	2.18	2.00	1.78	1.59	1.58	1.46	1.35	1.28
	$s_1/c\times10^2$	4.95	4.65	4.60	4.55	4.60	4.65	4.73	4.94	5.16
	U_{sep}/U_o	1.58	1.77	1.93	2.11	2.32	2.50	2.71	2.88	3.05
	$R\theta_{sep}$	1560	1550	1550	1500	1510	1590	1600	1560	1580
	$R_L\times10^{-3}$	60.1	74.2	81.1	75.9	71.9	64.3	57.6	49.5	43.9
	s_p/s_1	0.452	0.310	0.226	0.220	0.217	0.237	0.240	0.210	0.182
6.0	$L/c\times10^2$	0.35	0.75	0.75	0.67	0.55	0.45	0.37	0.26	0.22
	$^a(\delta/c)_{sep}\times10^4$	1.99	1.78	1.63	1.43	1.30	1.27	1.18	1.09	1.04
	$s_1/c\times10^2$	4.95	4.65	4.60	4.55	4.60	4.65	4.73	4.94	5.16
	U_{sep}/U_o	1.58	1.78	1.97	2.14	2.33	2.53	2.75	2.93	3.08
	$R\theta_{sep}$	1910	1910	1900	1830	1850	1950	1970	1920	1930
	$R_L\times10^{-3}$	33.4	80.0	87.1	85.6	76.9	68.3	60.7	45.6	40.4
	s_p/s_1	0.452	0.310	0.226	0.220	0.217	0.237	0.240	0.210	0.182
8.0	$L/c\times10^2$	0.05	0.50	0.58	0.53	0.43	0.33	0.24	---	---
	$^a(\delta/c)_{sep}\times10^4$	1.73	1.53	1.37	1.22	1.11	1.08	1.00	---	---
	$s_1/c\times10^2$	4.95	4.65	4.60	4.55	4.60	4.65	4.73	---	---
	U_{sep}/U_o	1.60	1.78	1.97	2.16	2.38	2.59	2.80	---	---
	$R\theta_{sep}$	2200	2180	2220	2140	2160	2270	2290	---	---
	$R_L\times10^{-3}$	6.5	71.3	92.3	91.6	81.9	68.3	53.8	---	---
	s_p/s_1	0.452	0.310	0.226	0.220	0.217	0.237	0.240	---	---
10.0	$L/c\times10^2$	0	0.40	0.48	0.45	---	---	---	---	---
	$^a(\delta/c)_{sep}\times10^4$	1.50	1.33	1.20	1.06	---	---	---	---	---
	$s_1/c\times10^2$	4.95	4.65	4.60	4.55	---	---	---	---	---
	U_{sep}/U_o	1.64	1.83	2.03	2.24	---	---	---	---	---
	$R\theta_{sep}$	2460	2480	2510	2420	---	---	---	---	---
	$R_L\times10^{-3}$	0	73.1	97.7	99.7	---	---	---	---	---
	s_p/s_1	0.452	0.310	0.226	0.220	---	---	---	---	---

(b) NACA 663-018 Airfoil

R, million	α, deg	7	8	9	10	11	12	13	14	15
1.5	$L/c\times10^2$	3.92	2.40	1.81	1.60	1.47	1.33	1.26	1.22	1.26
	$^a(\delta/c)_{sep}\times10^4$	2.80	2.50	2.34	2.27	2.14	1.98	1.88	1.77	1.73
	$s_1/c\times10^2$	5.23	5.35	5.49	5.70	5.88	6.12	6.37	6.58	6.90
	U_{sep}/U_o	1.75	1.91	2.08	2.15	2.26	2.46	2.58	2.70	2.73
	$R\theta_{sep}$	730	720	740	730	740	720	620	680	660
	$R_L\times10^{-3}$	103	68.4	56.4	51.6	49.9	48.9	48.8	49.5	51.6
	s_p/s_1	0.254	0.215	0.186	0.156	0.136	0.129	0.105	0.088	0.081
2.0	$L/c\times10^2$	2.72	1.73	1.38	1.20	1.10	0.99	0.95	0.94	0.92
	$(\delta/c)_{sep}\times10^4$	2.42	2.20	2.08	1.95	1.83	1.75	1.63	1.53	1.45
	$s_1/c\times10^2$	5.23	5.35	5.49	5.70	5.88	6.12	6.37	6.58	6.90
	U_{sep}/U_o	1.76	1.88	2.03	2.16	2.29	2.41	2.60	2.70	2.83
	$R\theta_{sep}$	850	830	840	840	840	840	850	830	820
	$R_L\times10^{-3}$	95.7	65.8	55.9	51.8	50.2	47.6	49.5	50.8	52.1
	s_p/s_1	0.254	0.215	0.186	0.156	0.136	0.129	0.105	0.088	0.081
3.0	$L/c\times10^2$	1.62	1.20	0.96	0.84	0.78	0.76	0.75	0.73	0.71
	$^a(\delta/c)_{sep}\times10^4$	1.88	1.75	1.65	1.54	1.42	1.37	1.29	1.21	1.13
	$s_1/c\times10^2$	5.23	5.35	5.49	5.70	5.88	6.12	6.37	6.58	6.90
	U_{sep}/U_o	1.84	1.93	2.09	2.23	2.38	2.52	2.68	2.80	2.95
	$R\theta_{sep}$	1070	1030	1040	1040	1050	1060	1050	1030	1020
	$R_L\times10^{-3}$	89.4	69.4	60.1	56.2	55.7	57.4	60.2	61.3	62.8
	s_p/s_1	0.258	0.237	0.204	0.175	0.148	0.127	0.108	0.094	0.081
4.0	$L/c\times10^2$	1.07	0.75	0.68	0.61	0.61	0.62	0.63	0.63	0.60
	$^a(\delta/c)_{sep}\times10^4$	1.65	1.50	1.42	1.32	1.22	1.17	1.11	1.02	0.98
	$s_1/c\times10^2$	5.23	5.35	5.49	5.70	5.88	6.12	6.37	6.58	6.90
	U_{sep}/U_o	1.82	1.95	2.10	2.26	2.41	2.57	2.70	2.85	2.97
	$R\theta_{sep}$	1230	1190	1200	1220	1220	1220	1230	1200	1180
	$R_L\times10^{-3}$	77.8	58.3	57.0	55.2	58.8	63.6	68.0	71.8	71.3
	s_p/s_1	0.274	0.234	0.195	0.167	0.146	0.126	0.105	0.093	0.081
6.0	$L/c\times10^2$	0.47	0.40	0.39	0.41	0.44	0.47	0.50	0.52	0.51
	$^a(\delta/c)_{sep}\times10^4$	1.33	1.20	1.14	1.07	0.99	0.94	0.89	0.81	0.76
	$s_1/c\times10^2$	5.23	5.35	5.49	5.70	5.88	6.12	6.37	6.58	6.90
	U_{sep}/U_o	1.85	2.00	2.14	2.28	2.45	2.59	2.76	2.90	3.12
	$R\theta_{sep}$	1510	1480	1500	1500	1500	1520	1510	1490	1500
	$R_L\times10^{-3}$	57.4	48.9	50.1	56.2	64.7	73.0	82.5	90.6	101.4
	s_p/s_1	0.279	0.234	0.204	0.169	0.150	0.131	0.113	0.096	0.081
8.0	$L/c\times10^2$	0.23	0.25	0.29	0.29	0.32	0.37	0.42	0.44	---
	$^a(\delta/c)_{sep}\times10^4$	1.14	1.03	0.97	0.90	0.84	0.79	0.75	0.70	---
	$s_1/c\times10^2$	5.23	5.35	5.49	5.70	5.88	6.12	6.37	6.58	---
	U_{sep}/U_o	1.86	2.02	2.17	2.33	2.51	2.67	2.82	2.96	---
	$R\theta_{sep}$	1750	1710	1750	1750	1750	1760	1770	1730	---
	$R_L\times10^{-3}$	34.2	40.2	50.4	54.2	64.0	78.8	94.4	104.0	---
	s_p/s_1	0.268	0.234	0.200	0.175	0.150	0.127	0.108	0.094	---
10.0	$L/c\times10^2$	0.07	0.11	0.20	0.25	---	---	---	---	---
	$^a(\delta/c)_{sep}\times10^4$	1.00	0.89	0.85	0.78	---	---	---	---	---
	$s_1/c\times10^2$	5.23	5.35	5.49	5.70	---	---	---	---	---
	U_{sep}/U_o	1.89	2.07	2.23	2.40	---	---	---	---	---
	$R\theta_{sep}$	1970	1930	1960	1980	---	---	---	---	---
	$R_L\times10^{-3}$	13.2	22.8	44.5	59.6	---	---	---	---	---
	s_p/s_1	0.279	0.237	0.195	0.170	---	---	---	---	---

[a] Calculated values based on measurements for $R = 2.0\times10^6$ and assuming that $(\delta/s_1)_{sep}$ varies inversely with $(U_{sep}/U_o)\sqrt{Rs_1}$

TABLE IV.- SUMMARY OF DATA FOR TURBULENCE LEVEL OF APPROXIMATELY 1.1 PERCENT (BASED ON THE ROOT-MEAN-SQUARE VALUE OF THE FLUCTUATING COMPONENT IN THE STREAMWISE DIRECTION) NACA 66_3-018 AIRFOIL

R, million	α, deg	7	8	9	10	11	12	13	14	15
1.5	$L/c \times 10^2$	1.45	1.16	0.97	0.95	0.93	0.89	0.87	0.81	0.76
	$s_l/c \times 10^2$	5.23	5.35	5.49	5.70	5.88	6.12	6.37	6.58	6.90
	U_{sep}/U_o	1.75	1.89	2.06	2.13	2.39	2.50	2.64	2.74	2.87
	$R_L \times 10^{-3}$	38.0	32.9	30.0	30.3	33.3	33.4	34.5	33.3	32.7
2.0	$L/c \times 10^2$	1.07	0.88	0.78	0.68	0.67	0.65	0.65	0.64	0.62
	$s_l/c \times 10^2$	5.23	5.35	5.49	5.70	5.88	6.12	6.37	6.58	6.90
	U_{sep}/U_o	1.84	1.95	2.10	2.24	2.43	2.54	2.62	2.82	2.93
	$R_L \times 10^{-3}$	39.4	34.3	32.8	30.5	32.5	33.0	34.0	36.1	36.3
3.0	$L/c \times 10^2$	0.67	0.53	0.48	0.47	0.48	0.48	0.49	0.49	0.48
	$s_l/c \times 10^2$	5.23	5.35	5.49	5.70	5.88	6.12	6.37	6.58	6.90
	U_{sep}/U_o	1.83	2.00	2.16	2.29	2.39	2.61	2.74	2.91	3.03
	$R_L \times 10^{-3}$	36.8	31.8	31.1	32.3	34.4	37.6	40.3	42.8	43.6
4.0	$L/c \times 10^2$	0.35	0.26	0.26	0.25	0.26	0.26	0.30	0.32	0.33
	$s_l/c \times 10^2$	5.23	5.35	5.49	5.70	5.88	6.12	6.37	6.58	6.90
	U_{sep}/U_o	1.84	1.98	2.14	2.30	2.44	2.58	2.79	2.92	3.08
	$R_L \times 10^{-3}$	25.7	20.6	22.3	23.0	25.4	26.8	33.5	27.3	40.7

A-17259

Figure 1.- The NACA 66_3-018 airfoil installed in the Ames 7- by 10-foot wind tunnel.

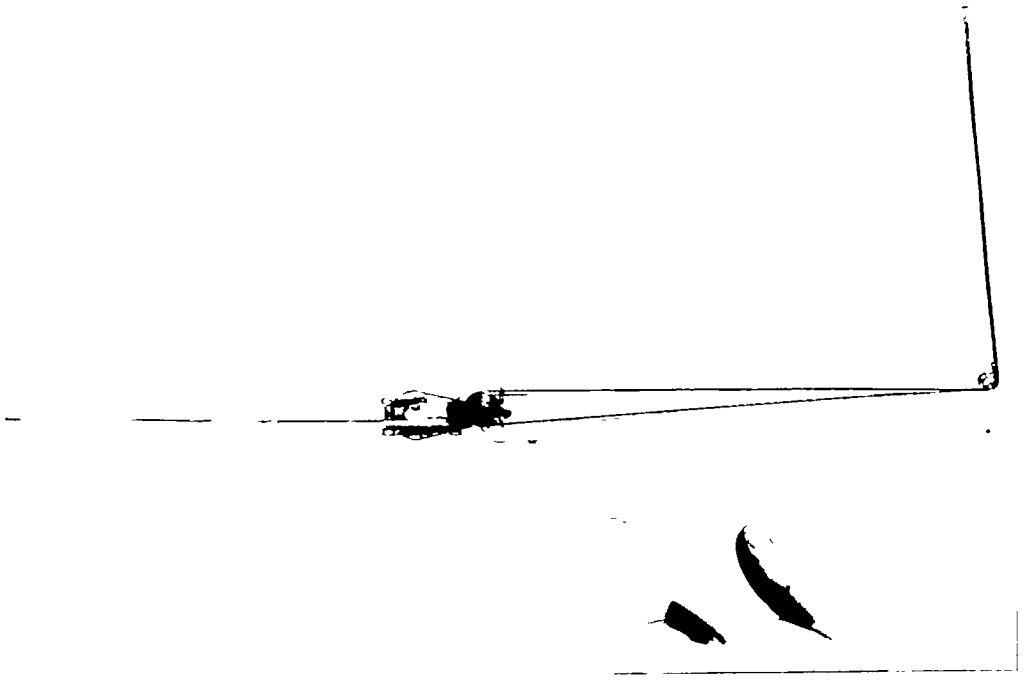

A-17260

(a) General view.

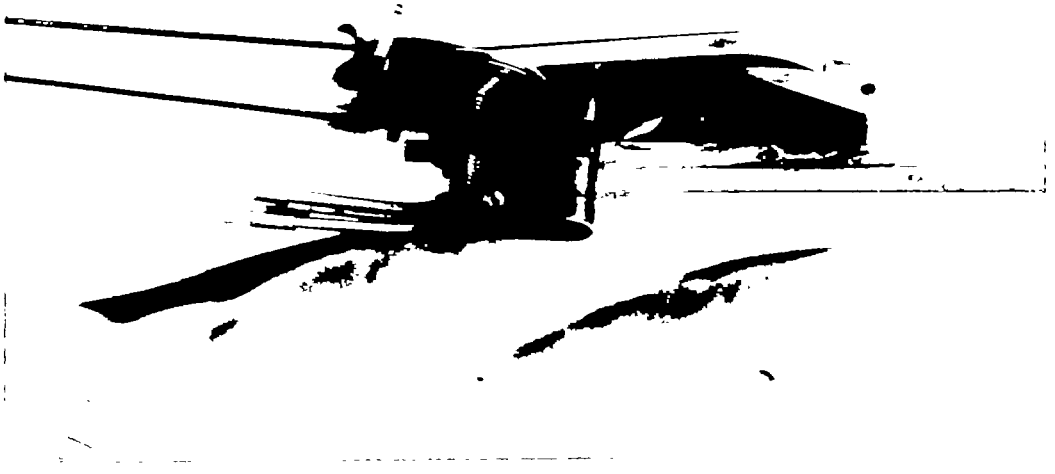

A-17261

(b) Detailed view.

Figure 2.- The boundary-layer-survey apparatus.

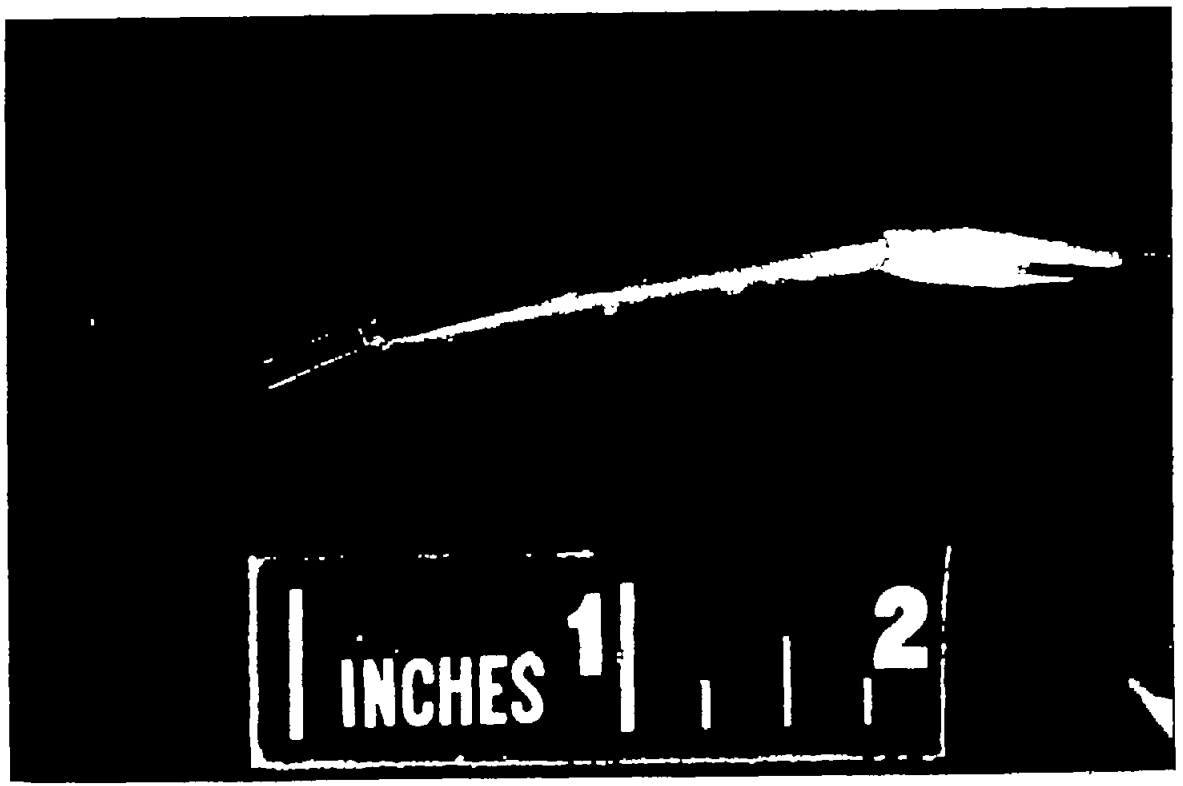

Figure 3.- The hot-wire anemometer probe. A-19041

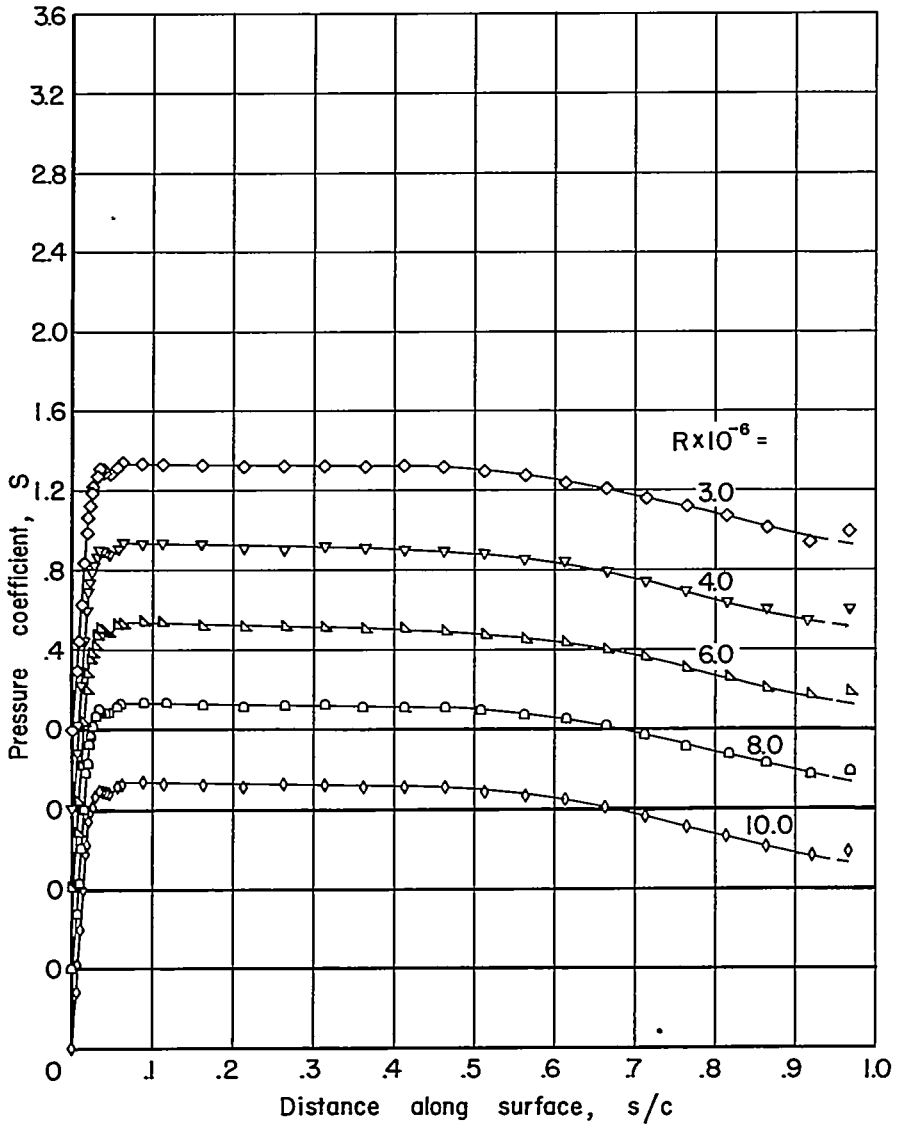

(a) $\alpha = 0^{\circ}$

Figure 4.- Typical pressure distributions for the NACA 0010 (modified) airfoil.

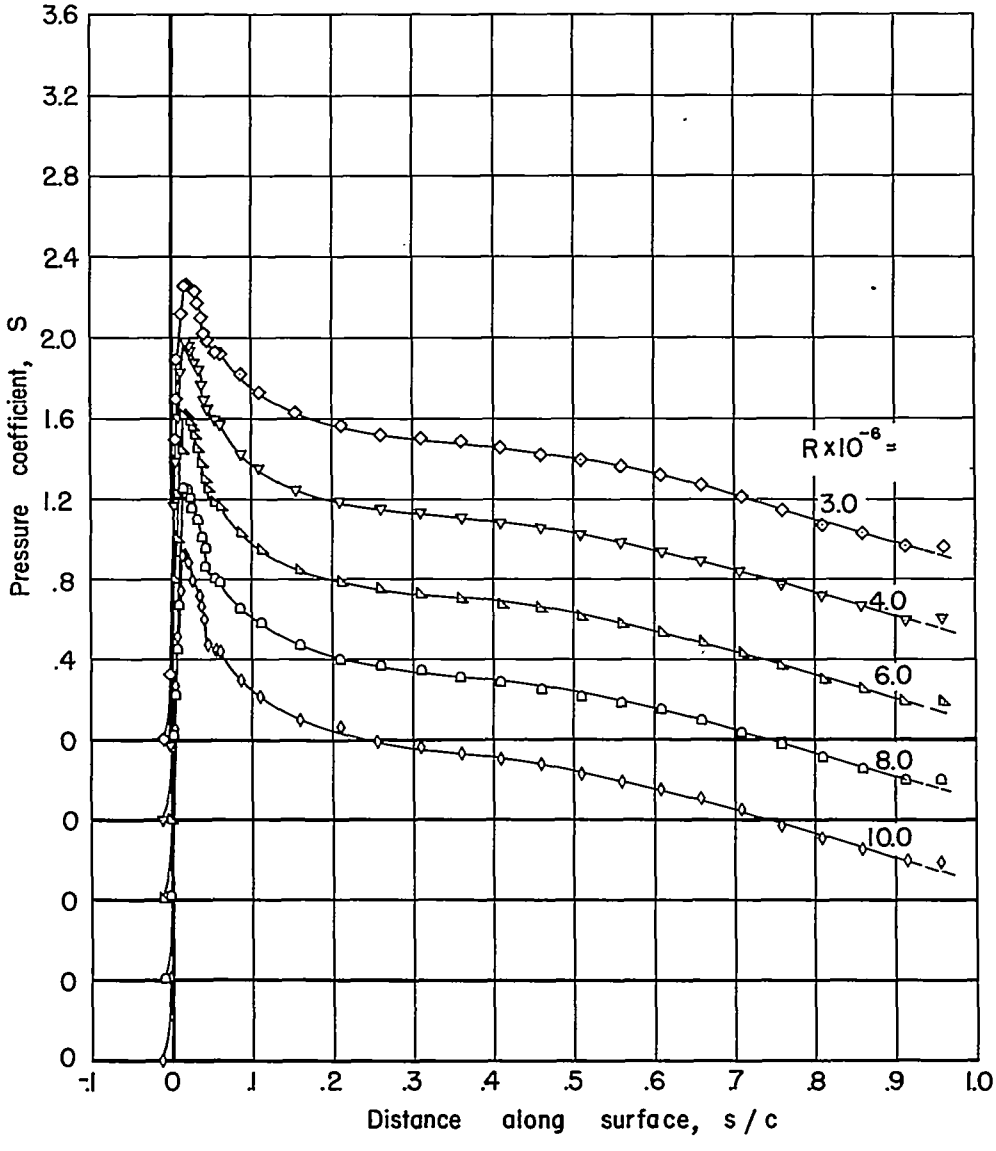

(b) $\alpha = 3^{\circ}$

Figure 4.- Continued.

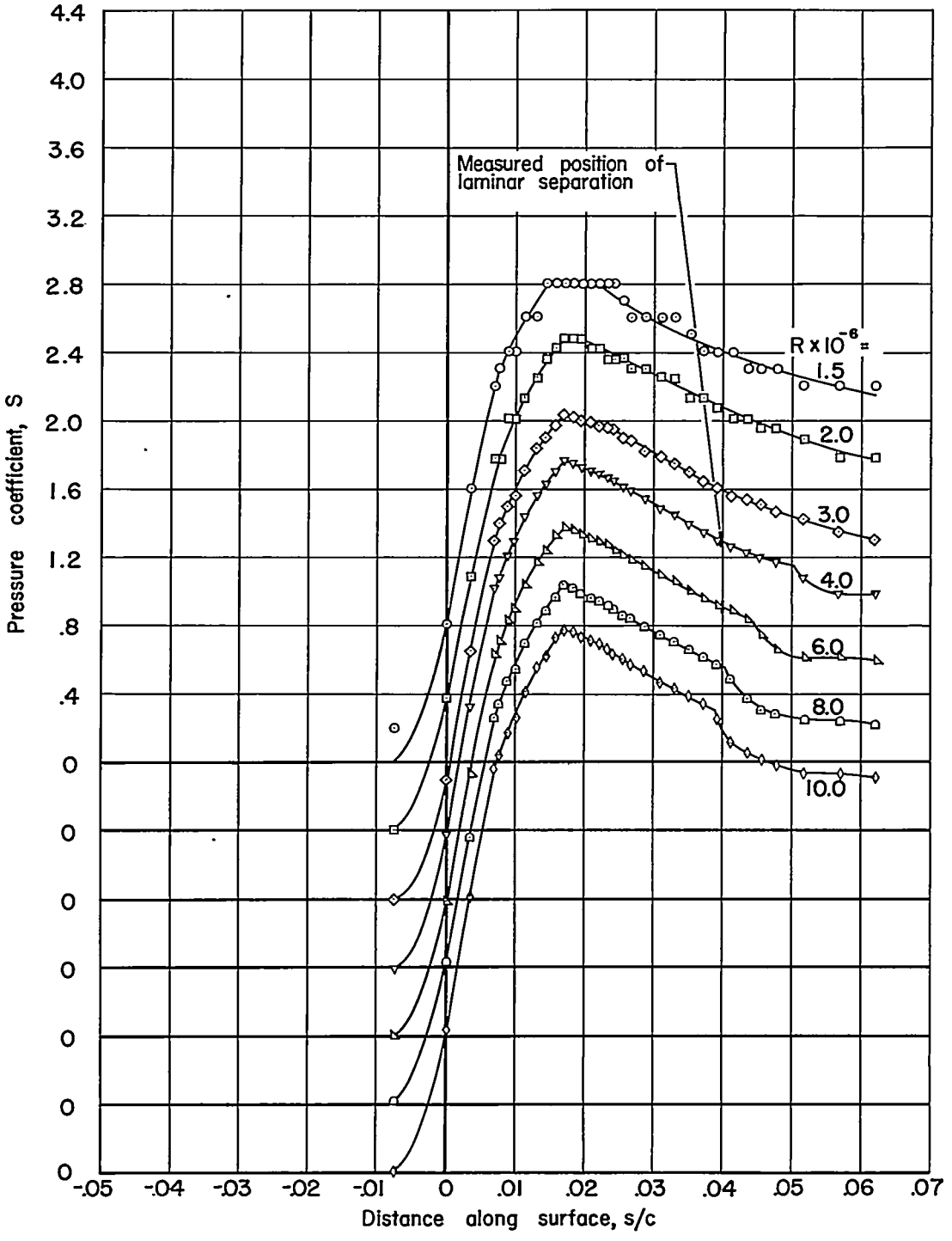

(c) $\alpha = 4^{\circ}$

Figure 4.- Continued.

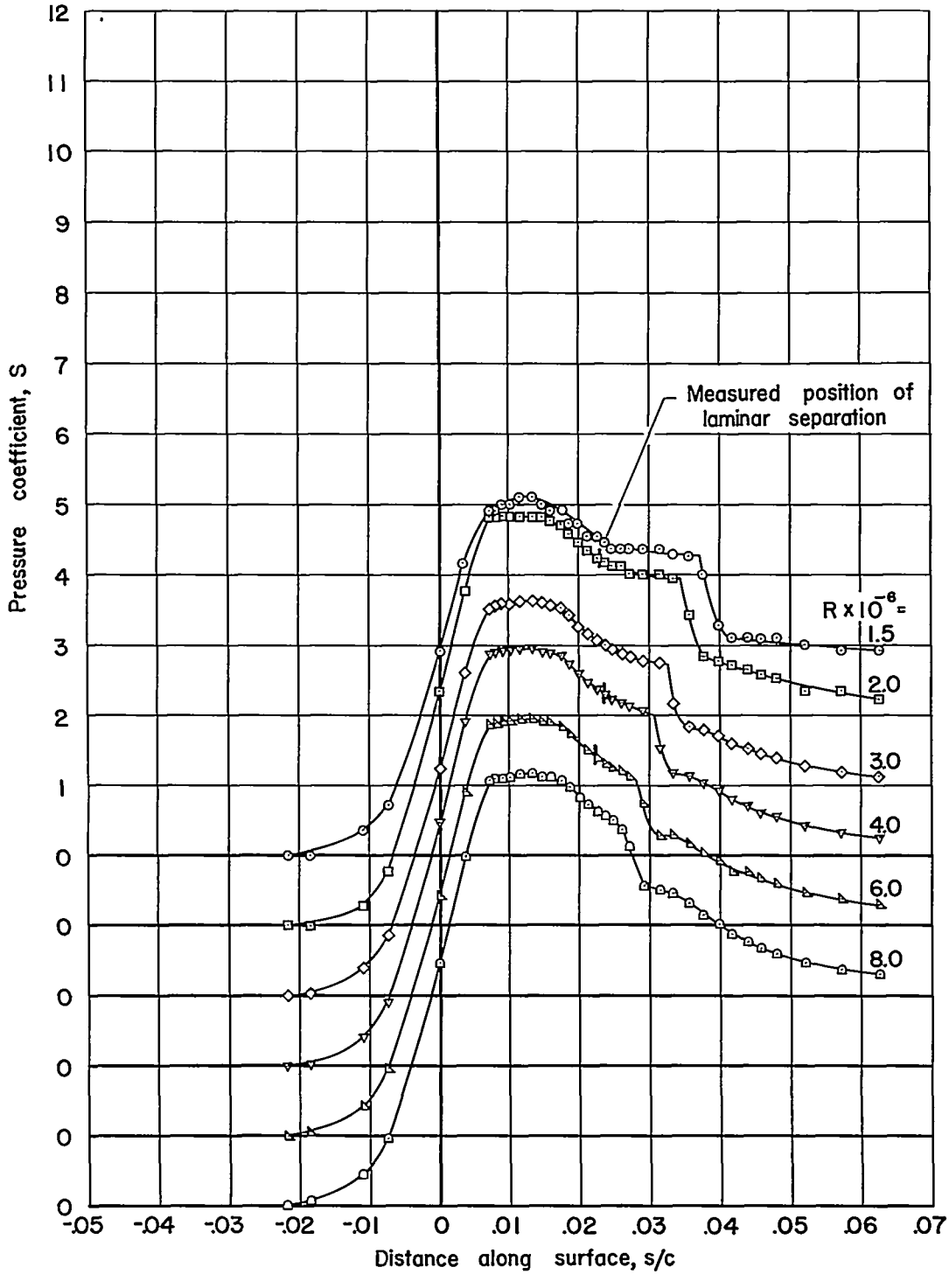

(d) $\alpha = 8^{\circ}$

Figure 4.- Continued.

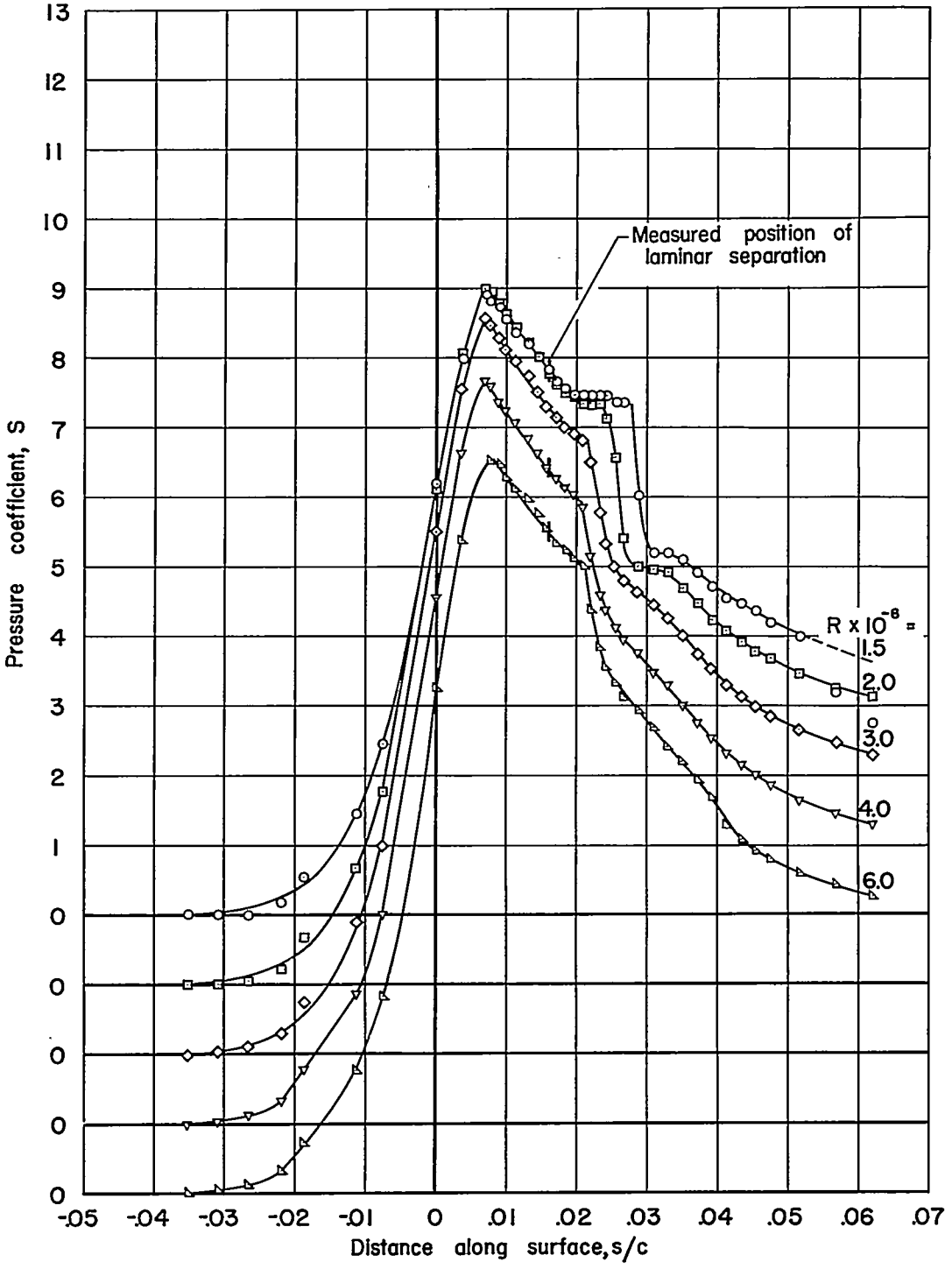

(e) $\alpha = 12^{\circ}$

Figure 4.- Concluded.

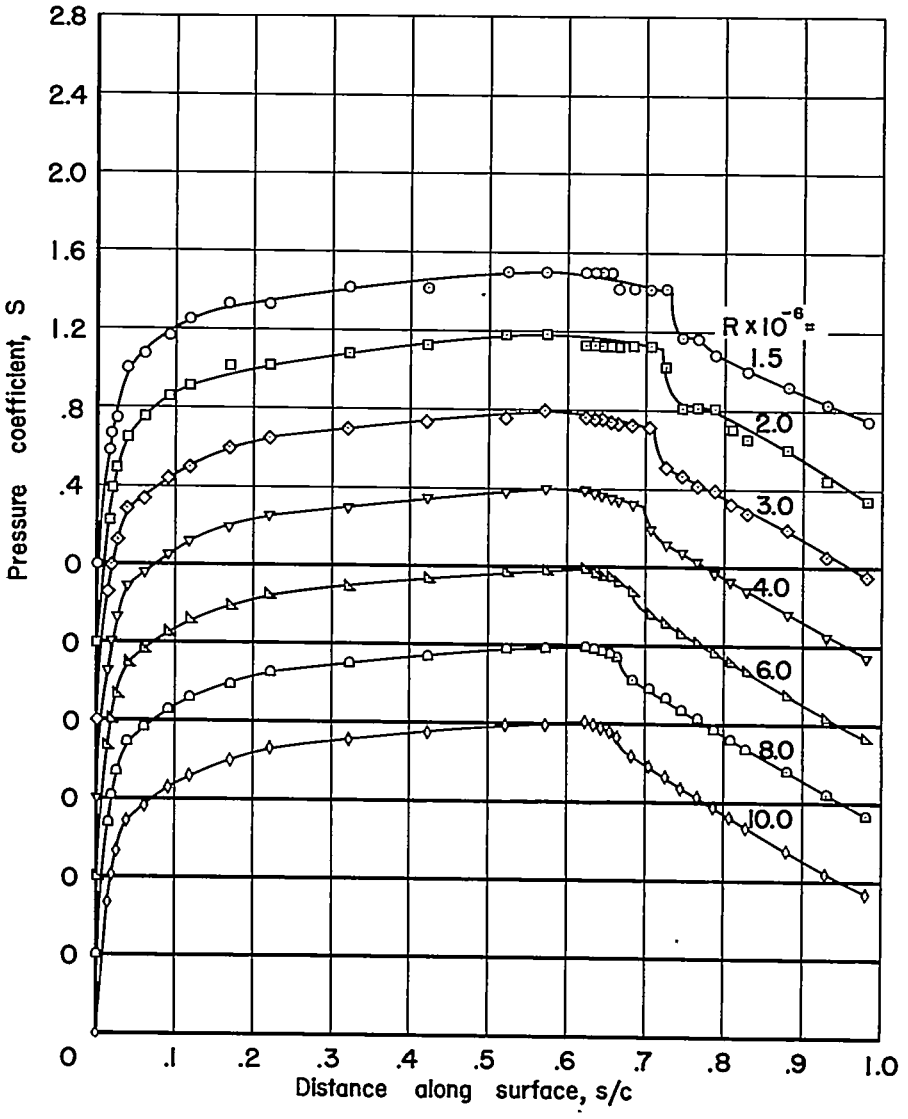

(a) $\alpha = 0^{\circ}$

Figure 5.- Typical pressure distributions measured near the midchord and leading edge of the NACA 663-018 airfoil.

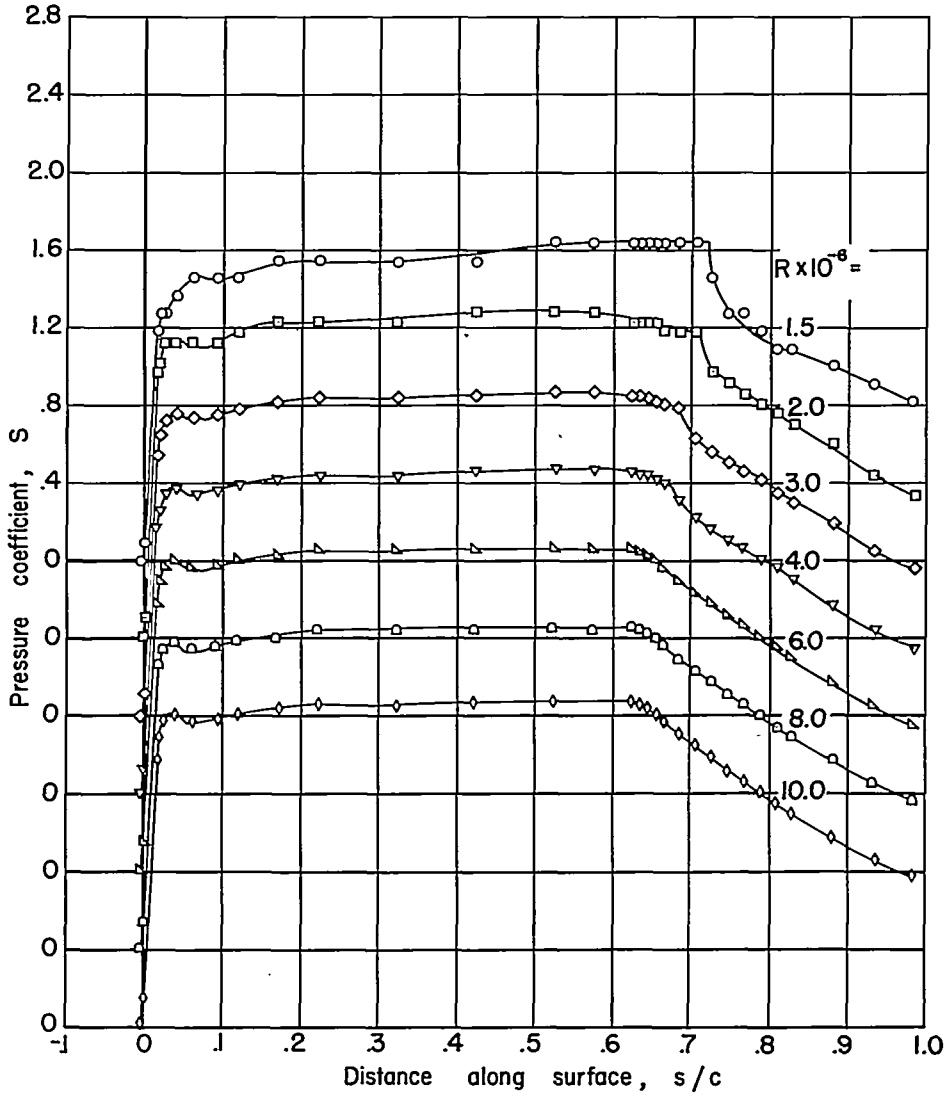

(b) $\alpha = 2^{\circ}$

Figure 5.- Continued.

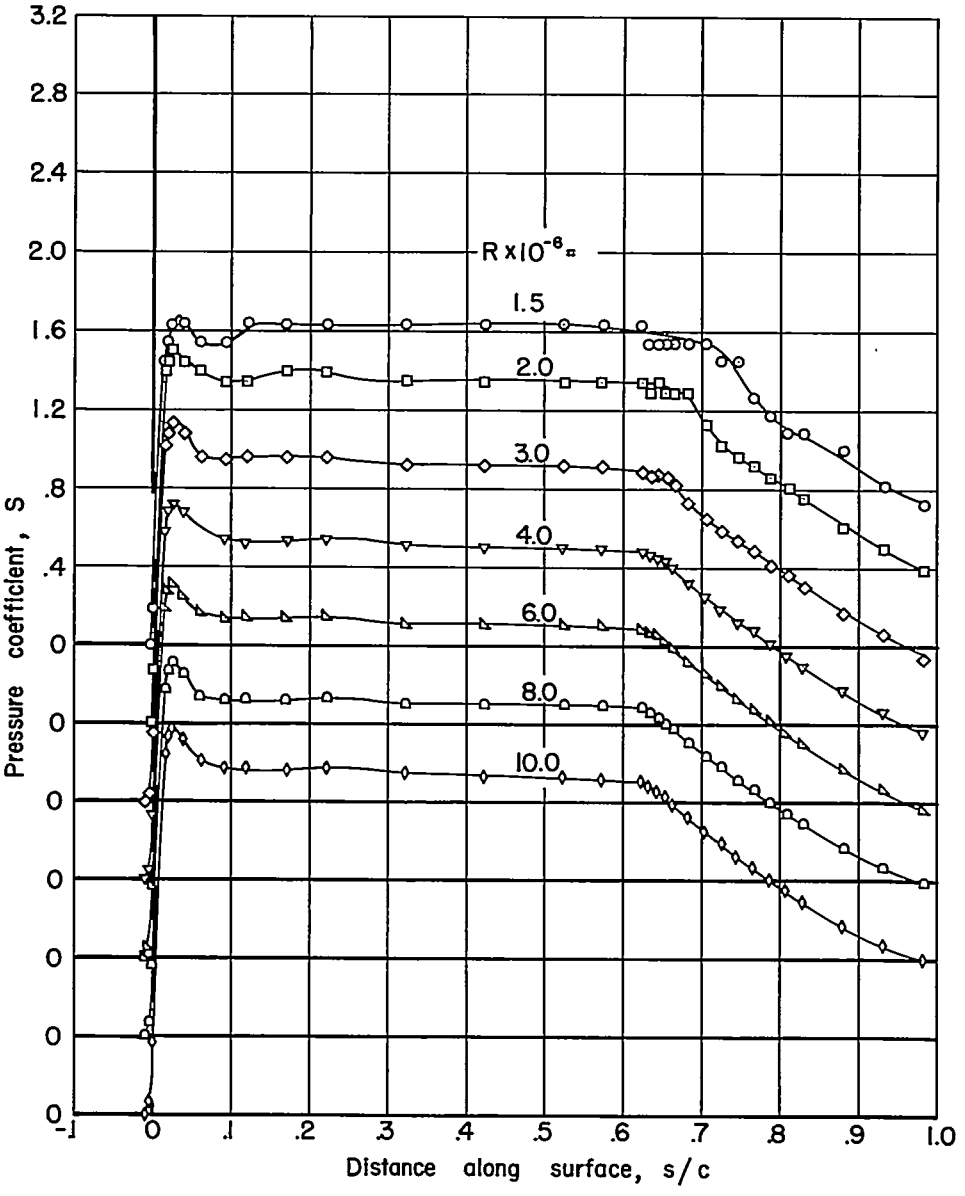

(c) $\alpha = 3^{\circ}$

Figure 5.- Continued.

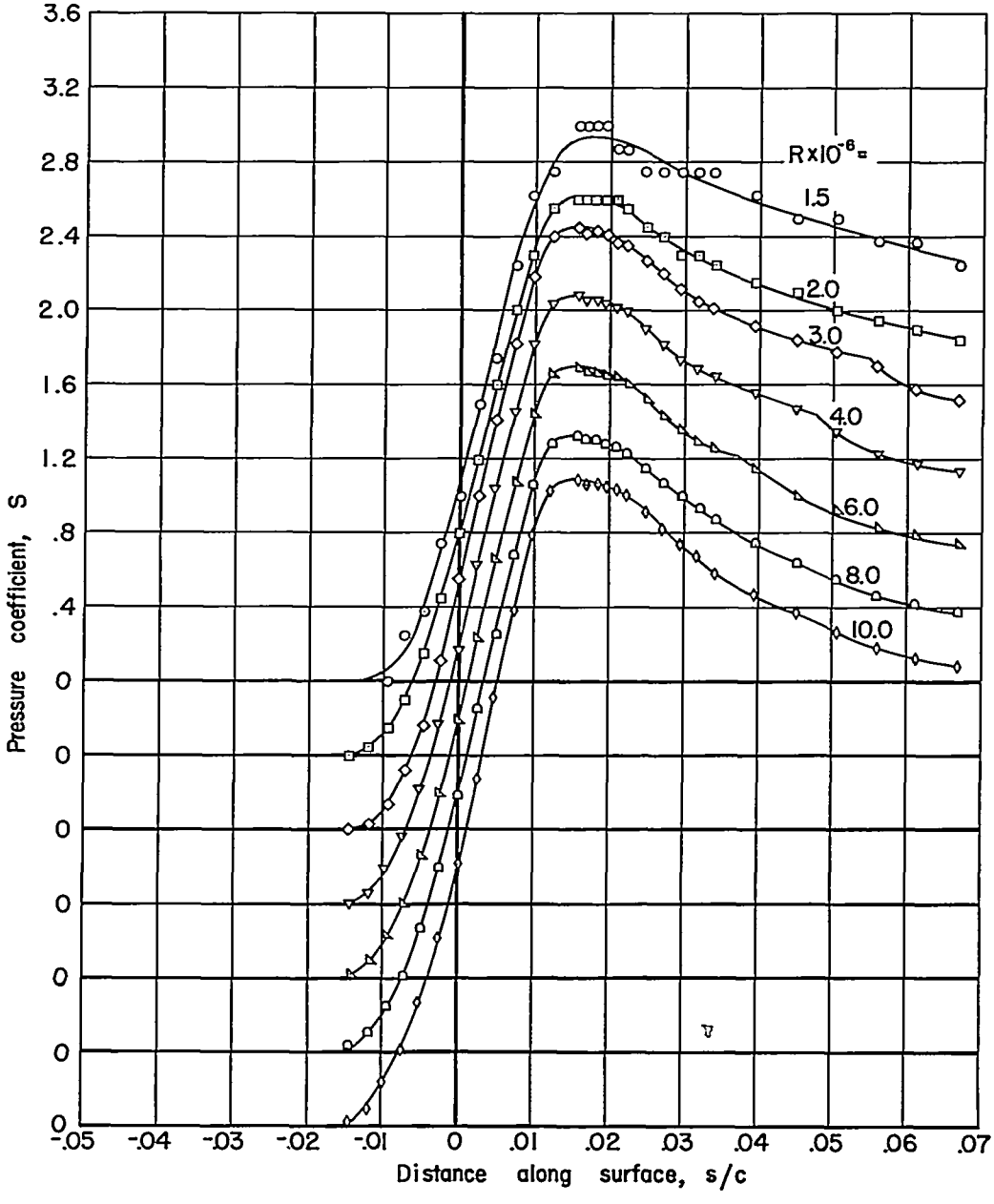

(d) $\alpha = 6^{\circ}$

Figure 5.- Continued.

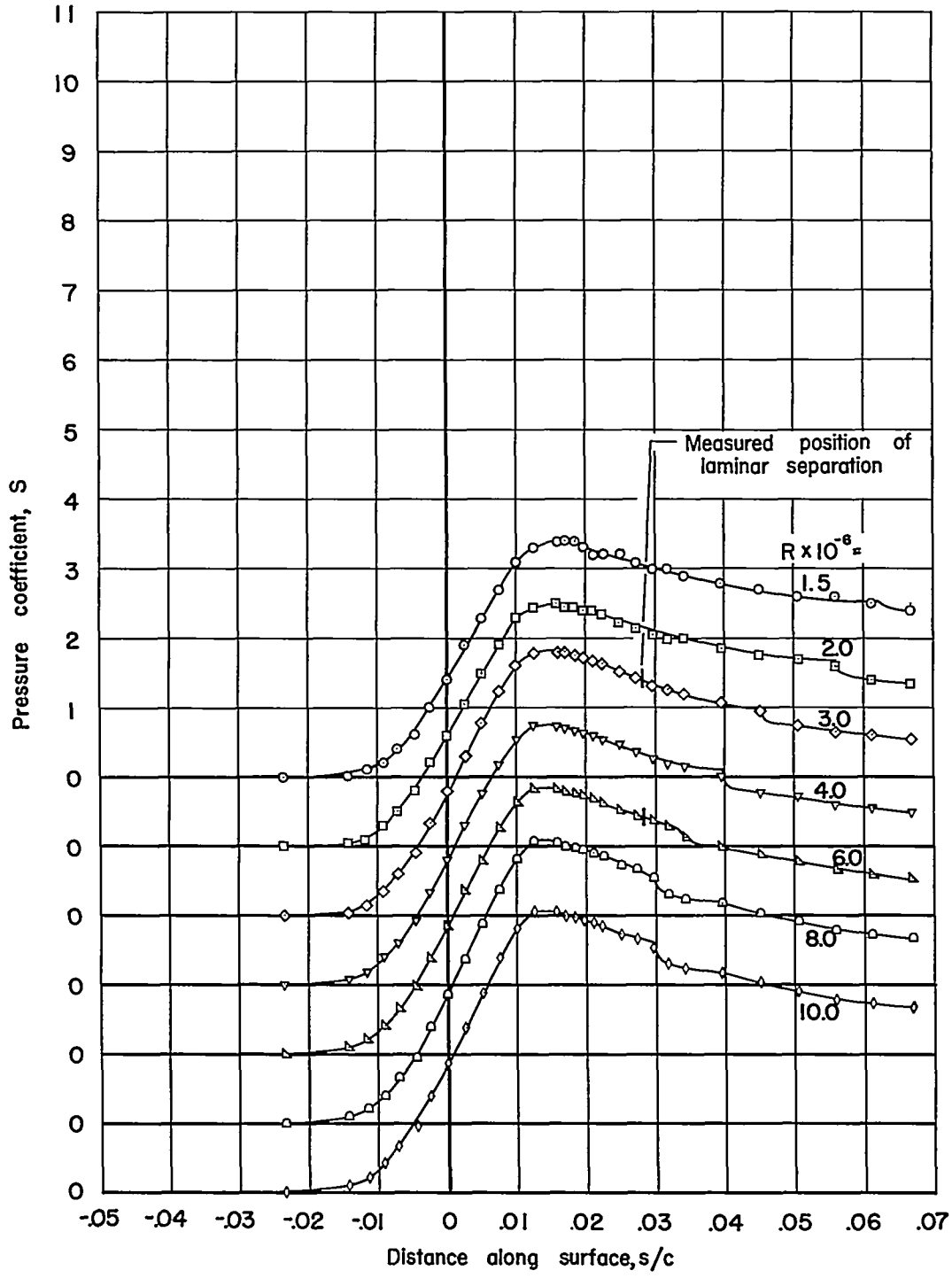

(e) $\alpha = 7^{\circ}$

Figure 5.- Continued.

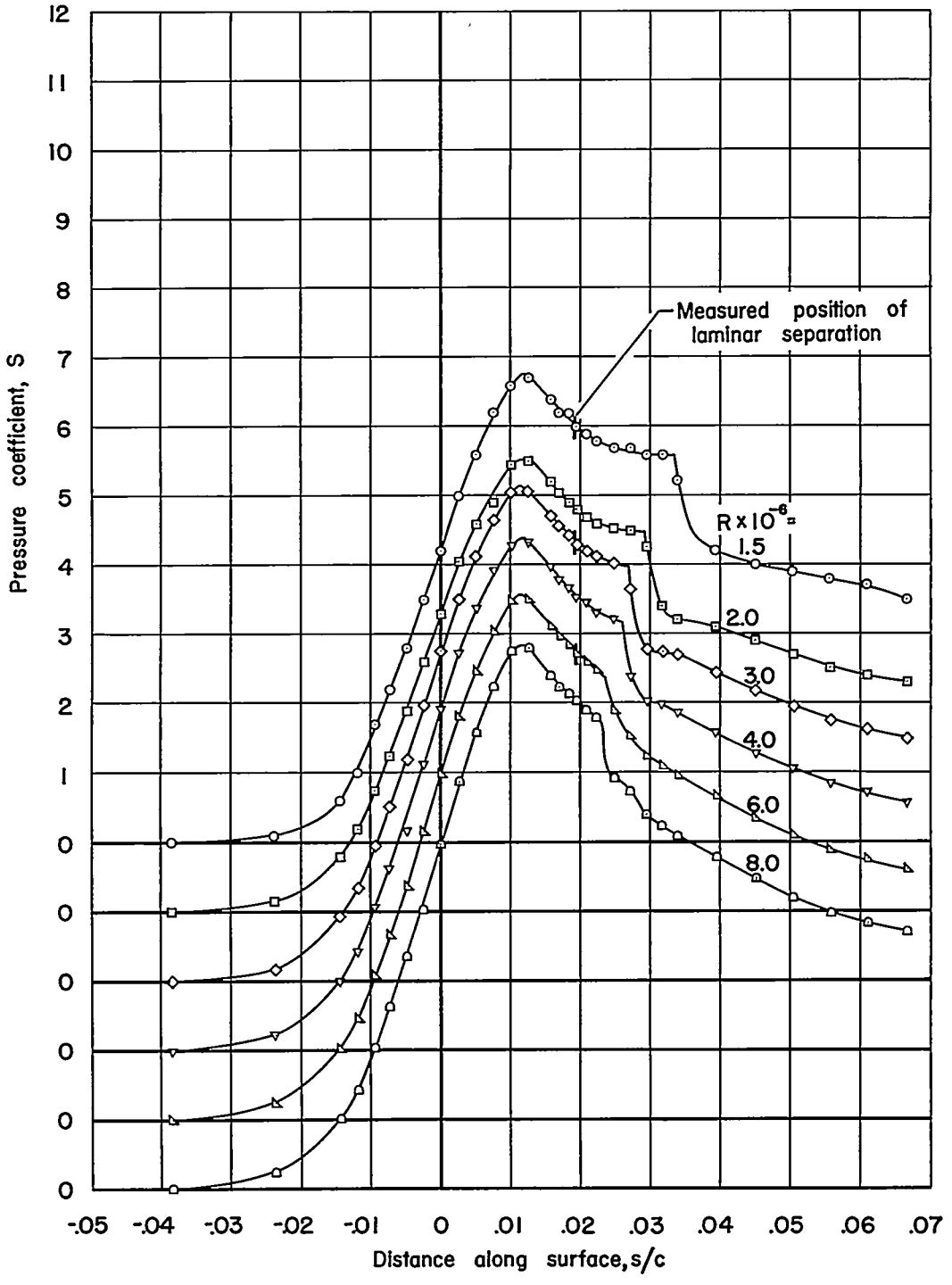

(f) $\alpha = 12^{\circ}$

Figure 5.- Continued.

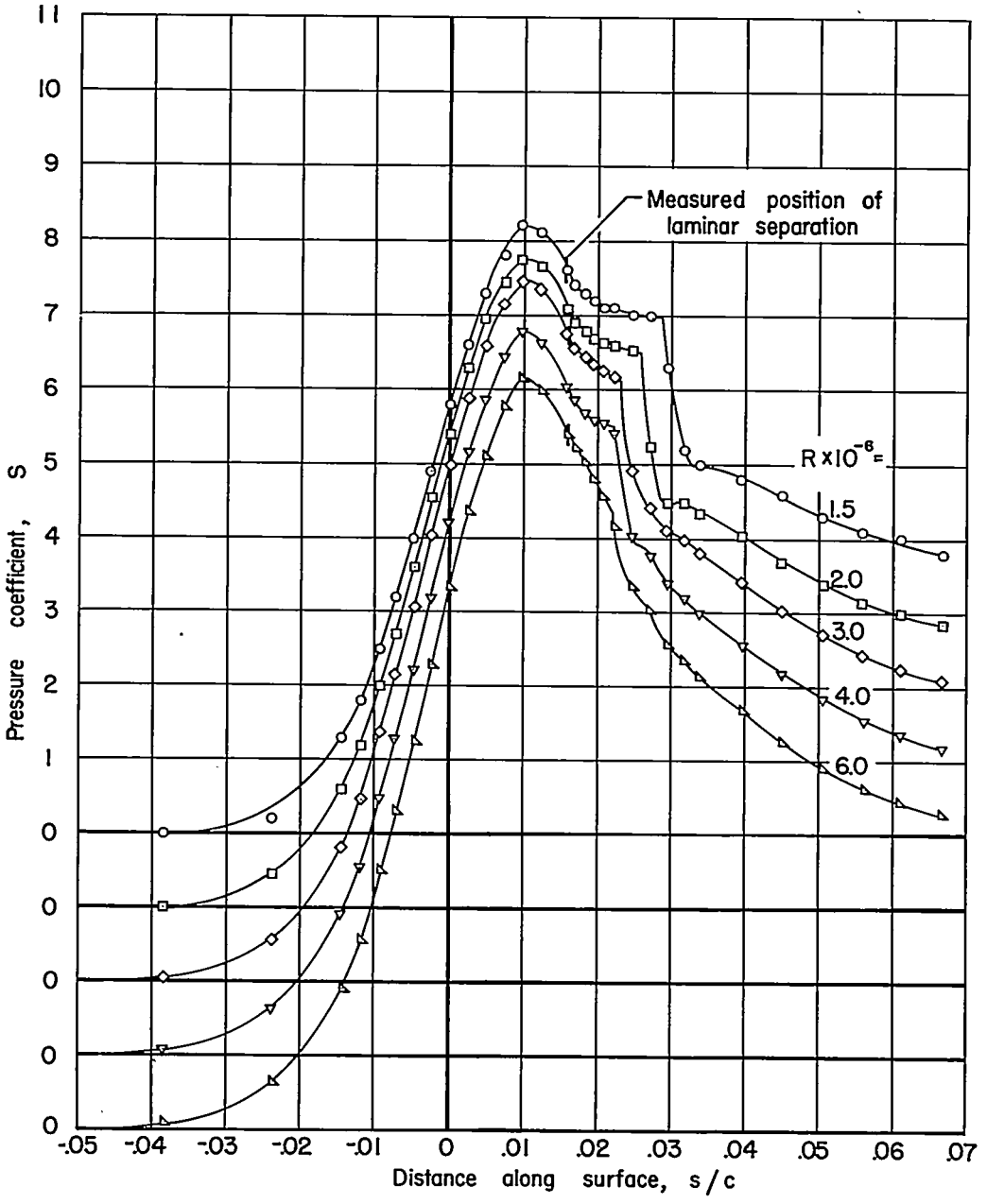

(g) $\alpha = 15^{\circ}$

Figure 5.- Concluded.

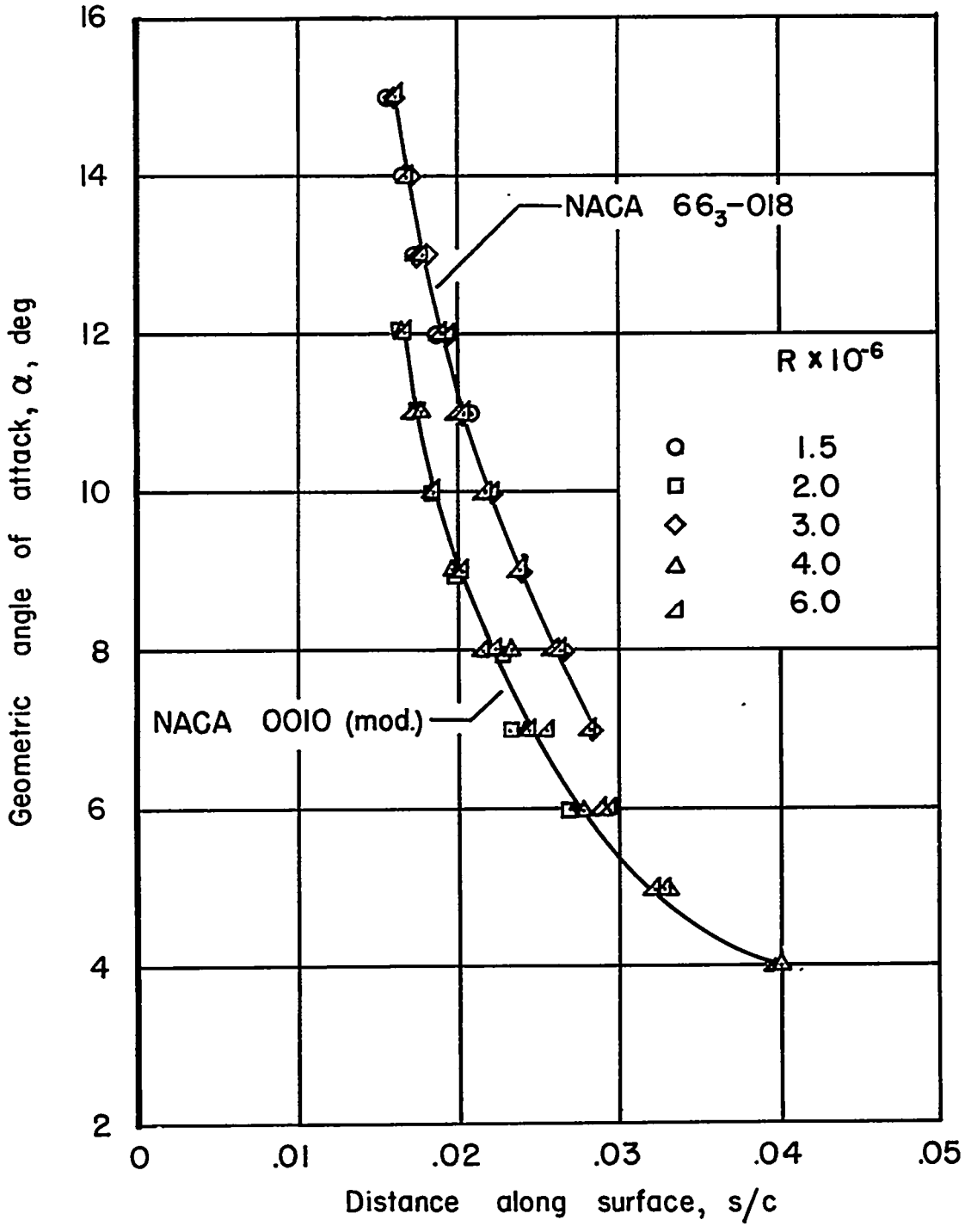

Figure 6.- The position of separation of the laminar boundary-layer flow as determined by liquid-film measurements.

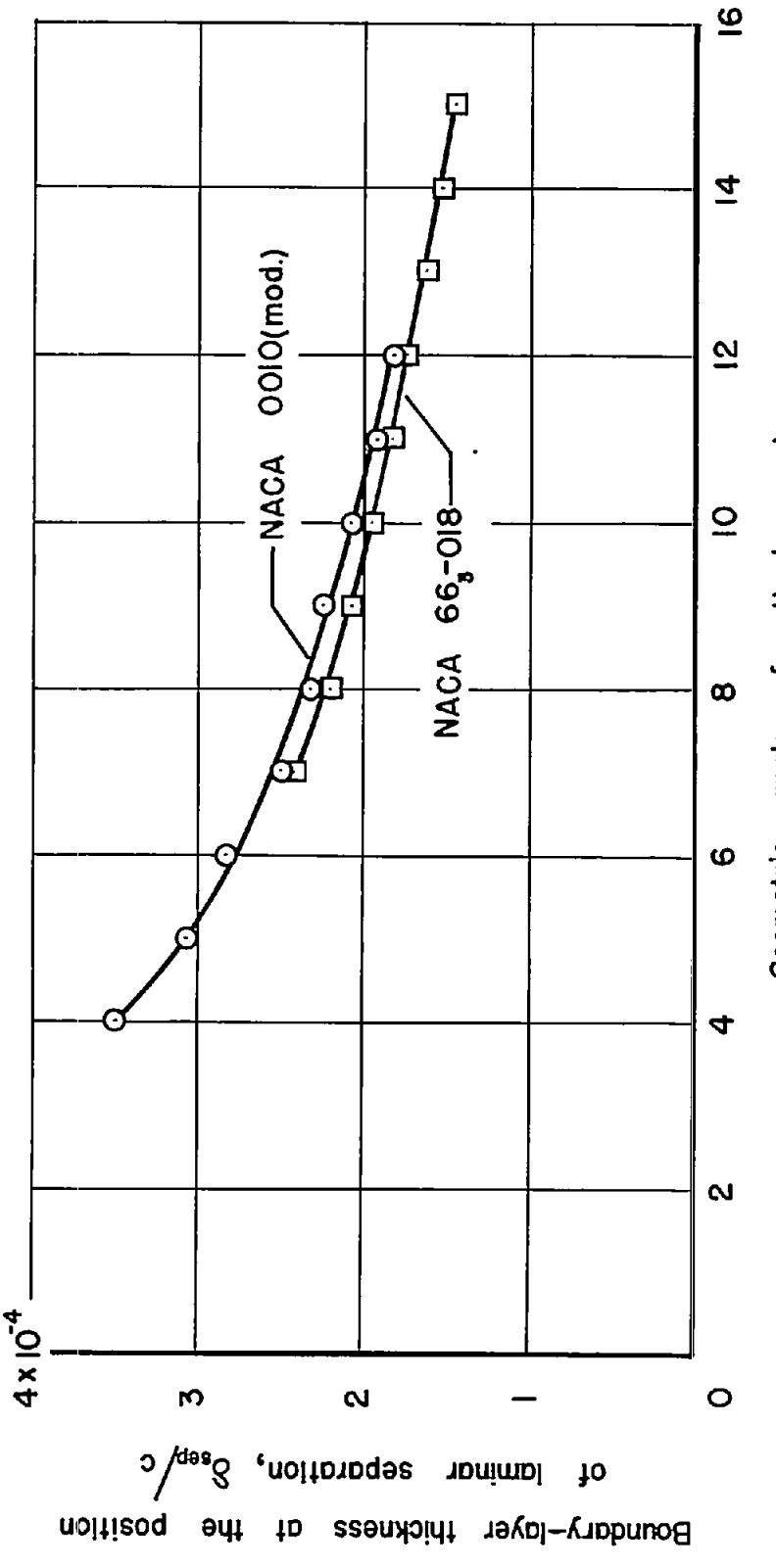

Figure 7.- The boundary-layer thickness at the position of laminar separation; R = 2×10^6.

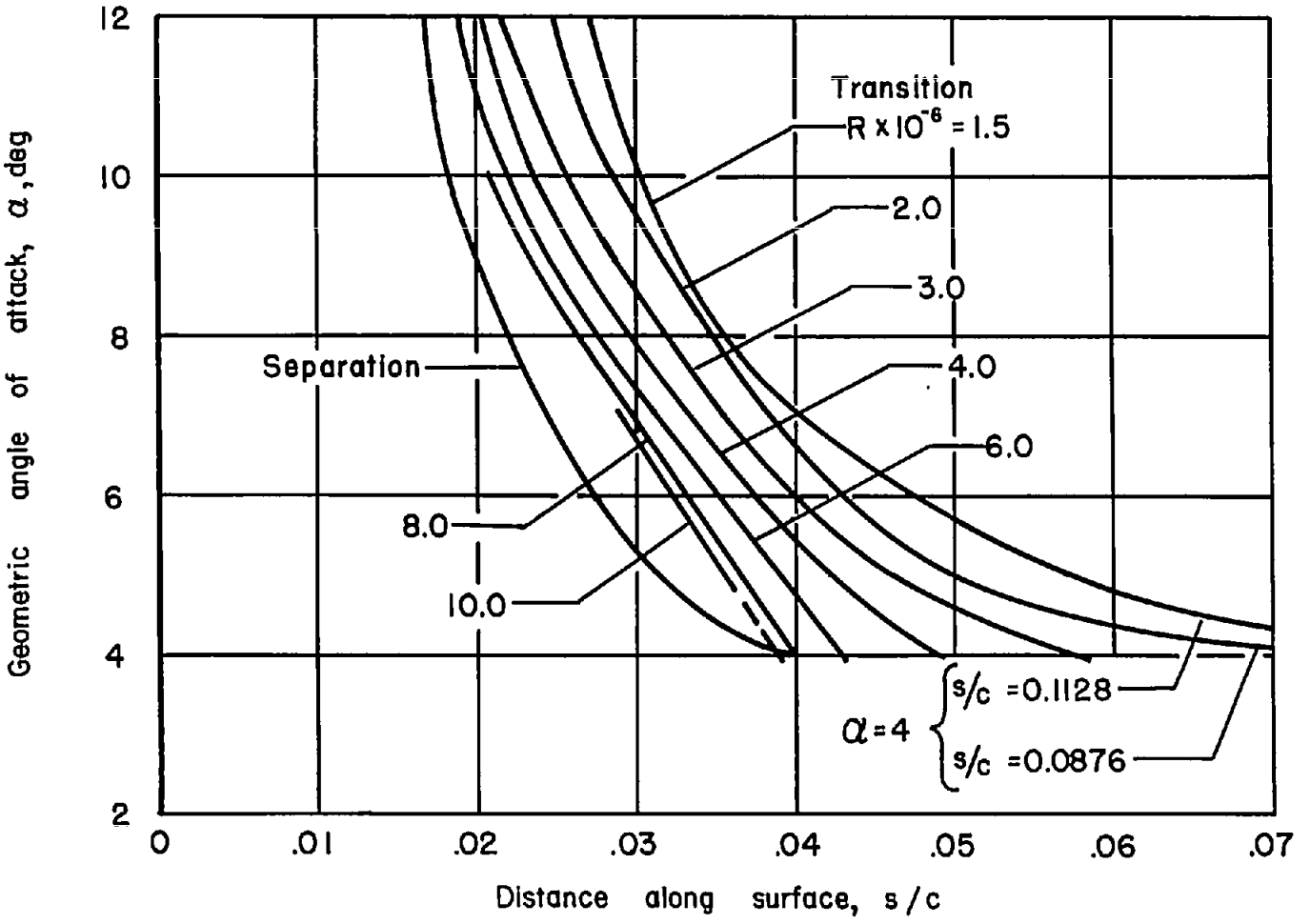

(a) Near the leading edge, NACA 0010 (modified).

Figure 8.- The position of transition from laminar to turbulent flow.

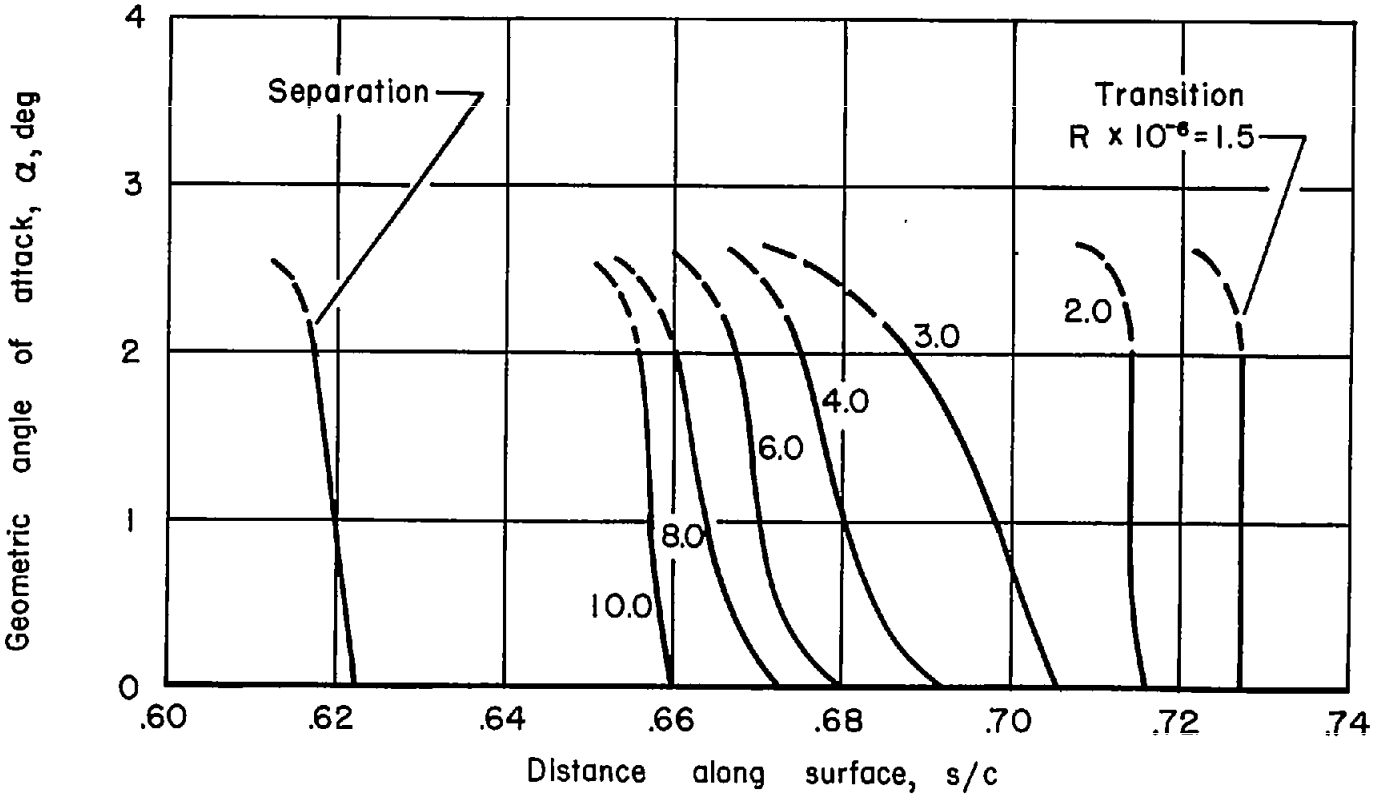

(b) Near midchord, NACA 663-018.

Figure 8.- Continued.

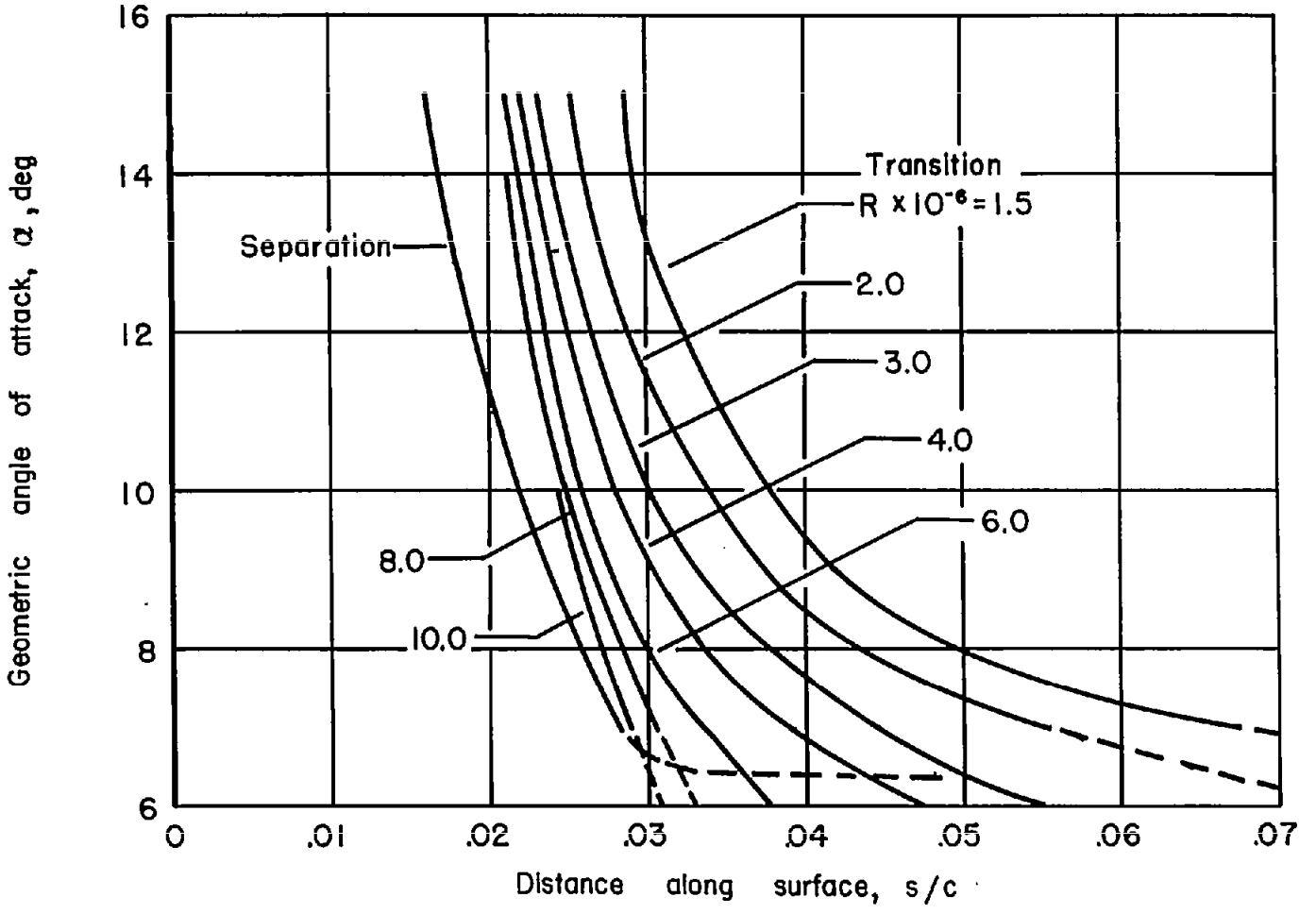

(c) Near leading edge, NACA 663-018.

Figure 8.- Concluded.

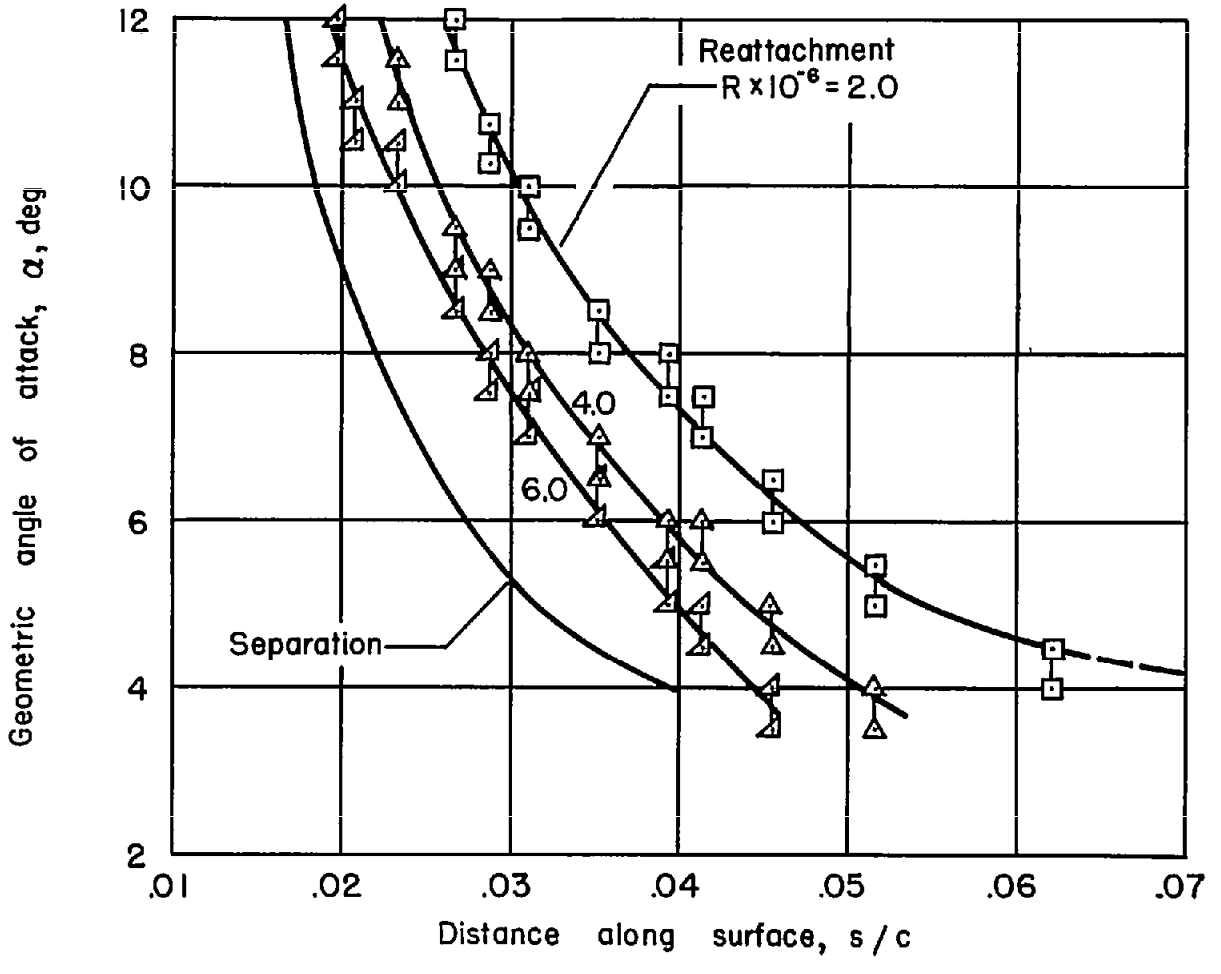

(a) NACA 0010 (modified).

Figure 9.- The position of flow reattachment.

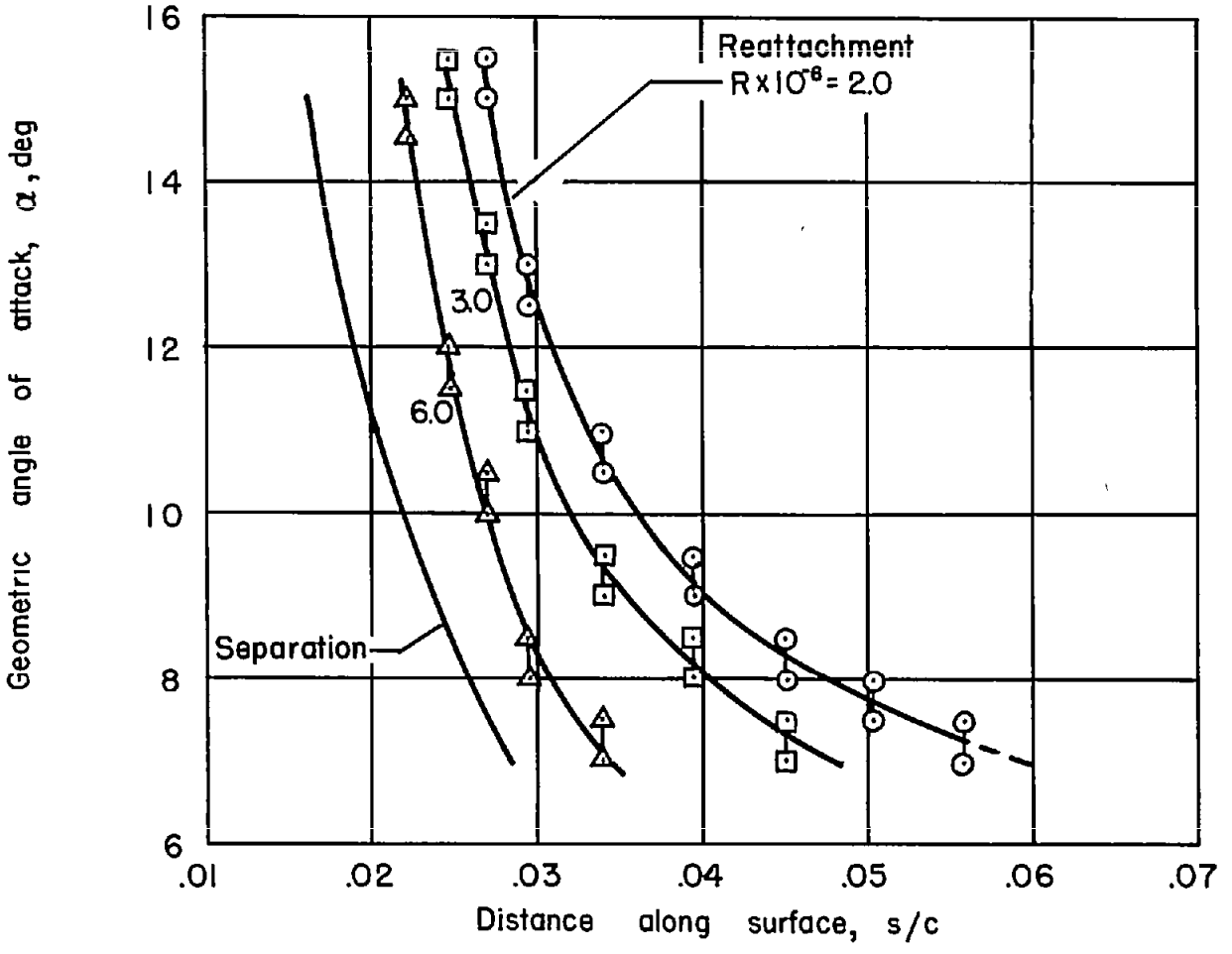

(b) NACA 663-018.

Figure 9.- Concluded.

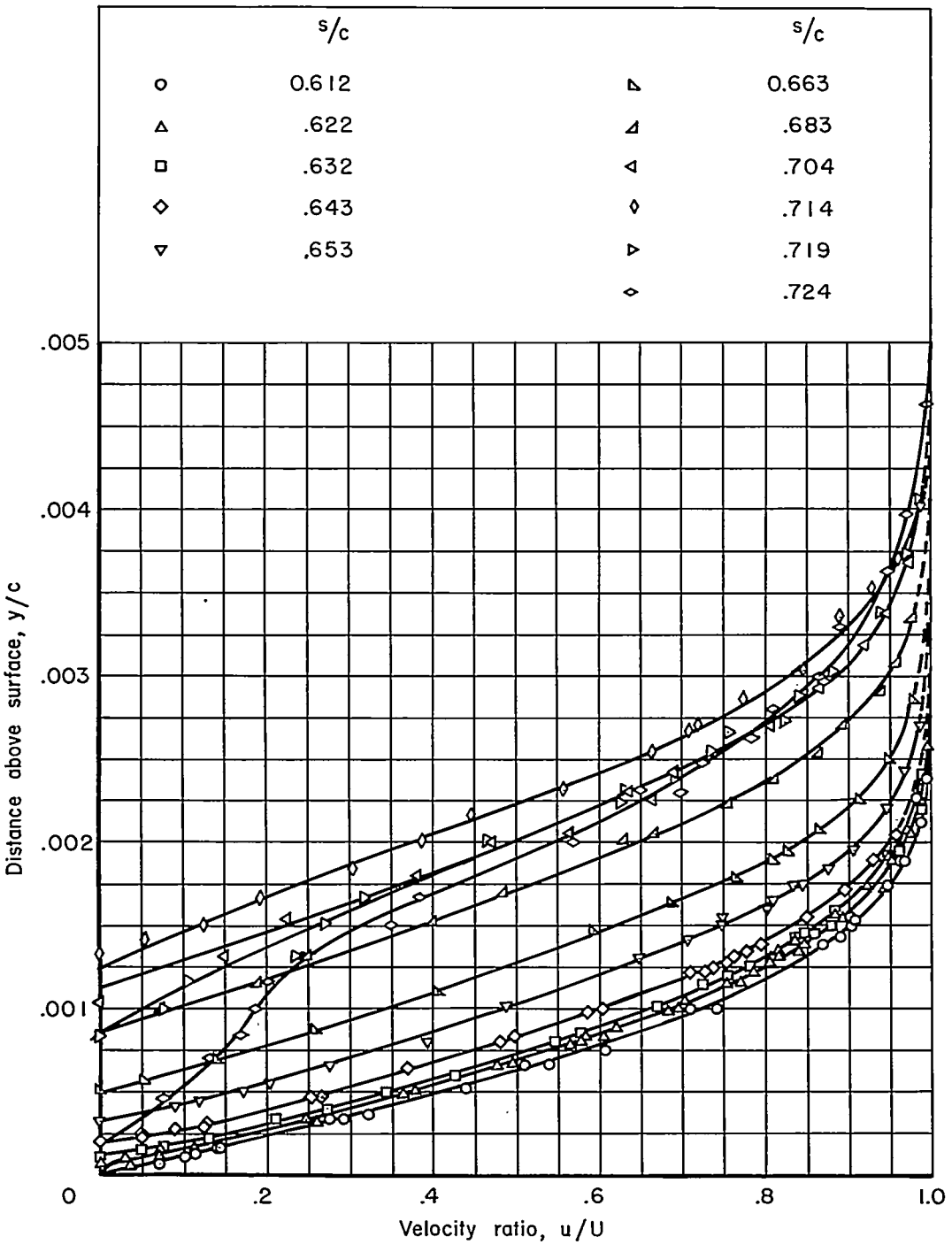

(a) $\alpha = 0^{\circ}$

Figure 10.- Boundary-layer velocity profiles near midchord on the NACA $663\text{-}018$ airfoil; $R = 2 \times 10^{6}$.

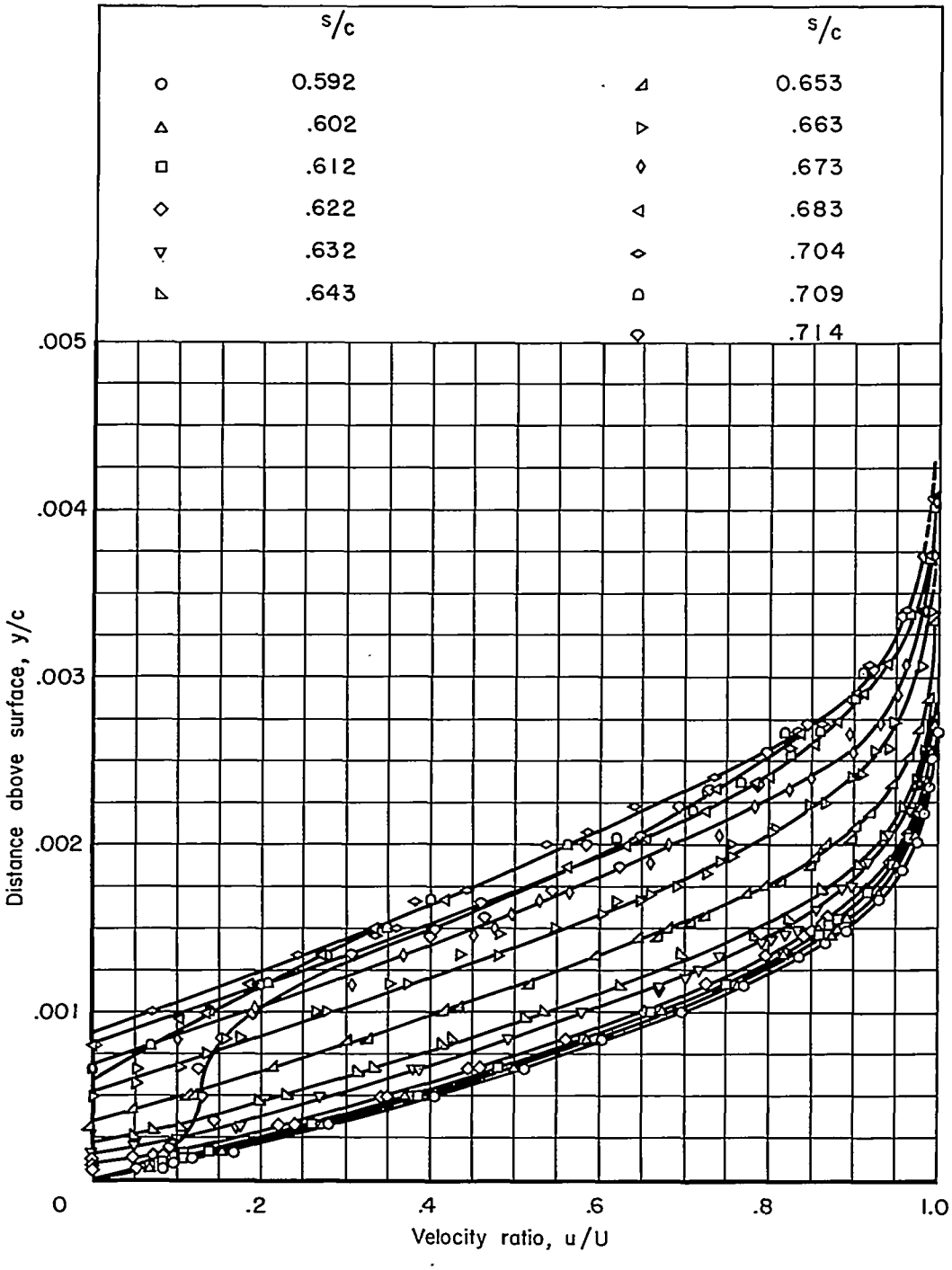

(b) $\alpha = 2^{\circ}$

Figure 10.- Concluded.

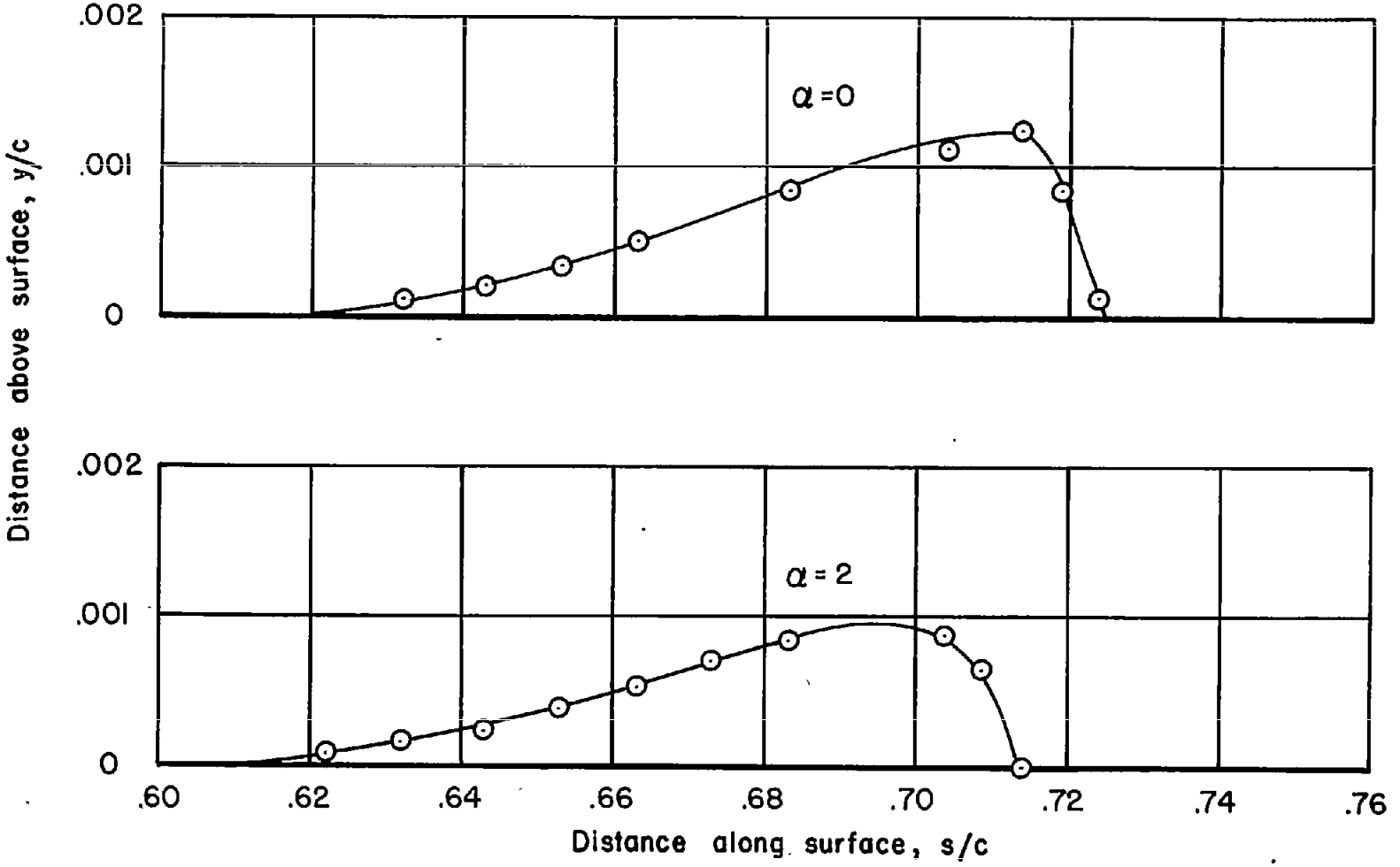

Figure 11.- The bubble shapes near midchord on the NACA 663-018 airfoil (the regions bounded by the airfoil surface and the contours along which the measured values of $u/U = 0$); $R = 2 \times 10^6$.

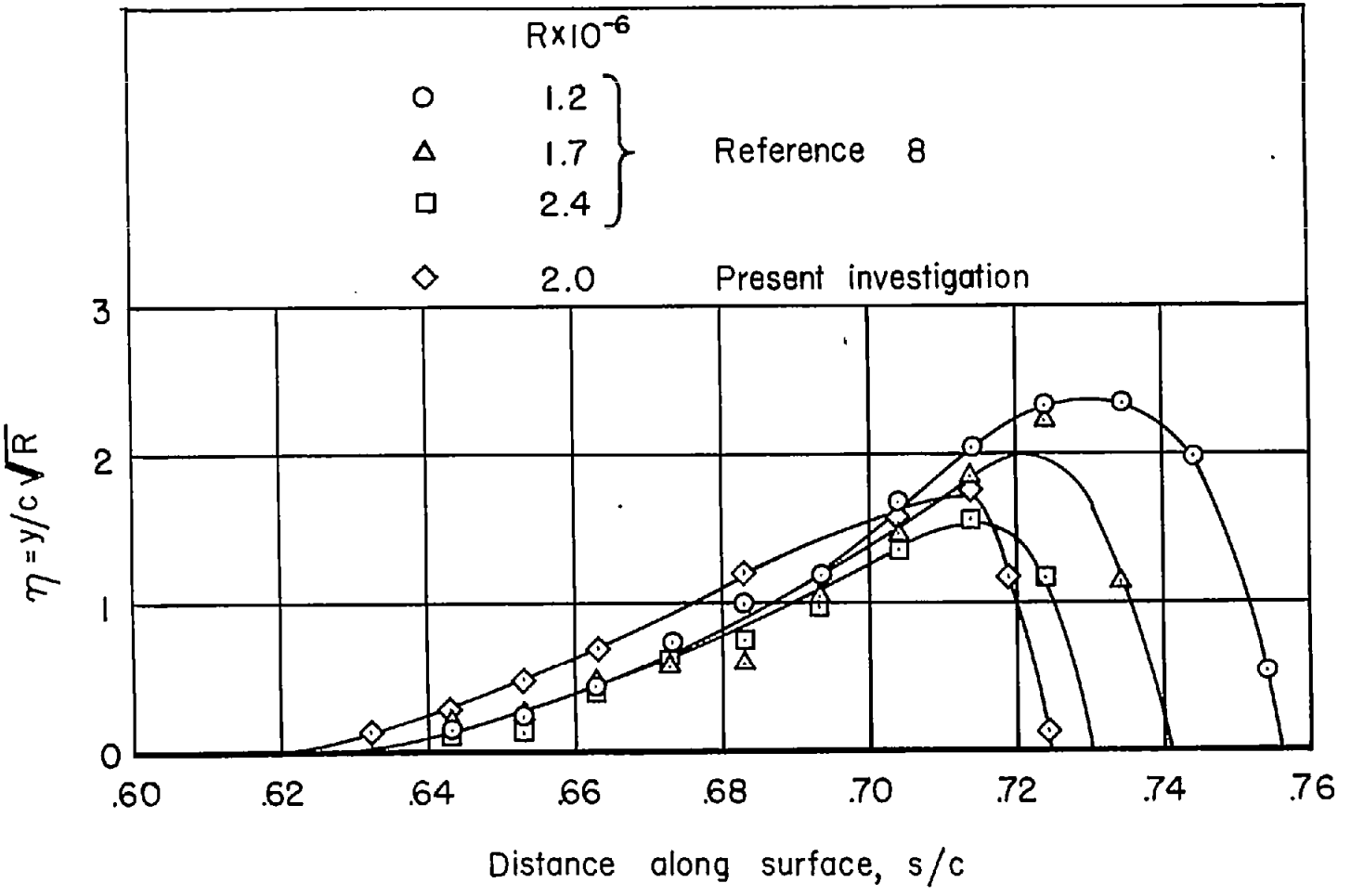

Figure 12.- Bubble shapes for $\alpha = 0$ near midchord for the NACA 663-018 airfoil as determined by the present investigation and reference 8 (regions bounded by the airfoil surface and the contours along which the measured values of $u/U = 0$).

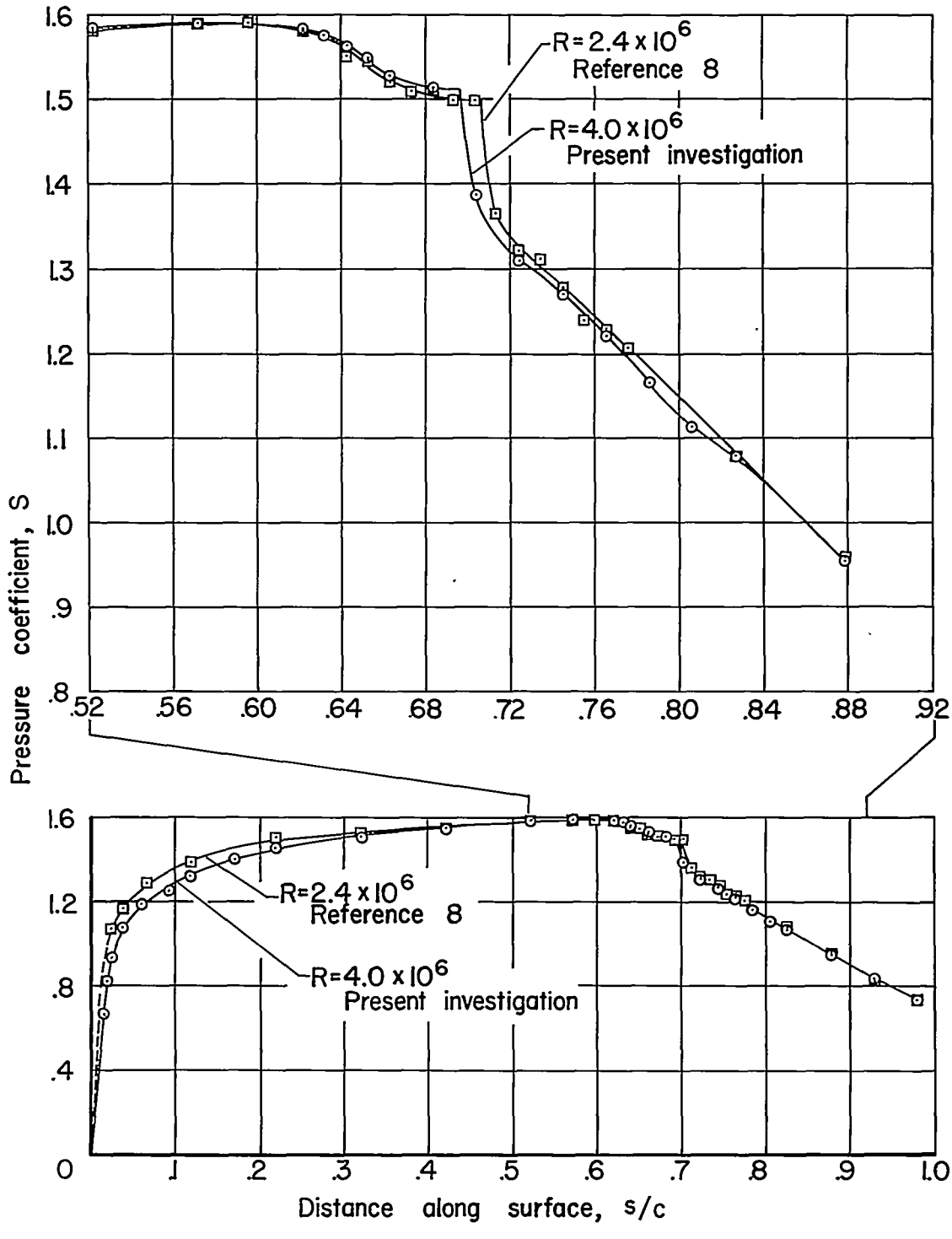

Figure 13.- Comparison of pressure distributions from reference 8 and present investigation for the NACA 66_3-018 airfoil; $\alpha = 0^\circ$.

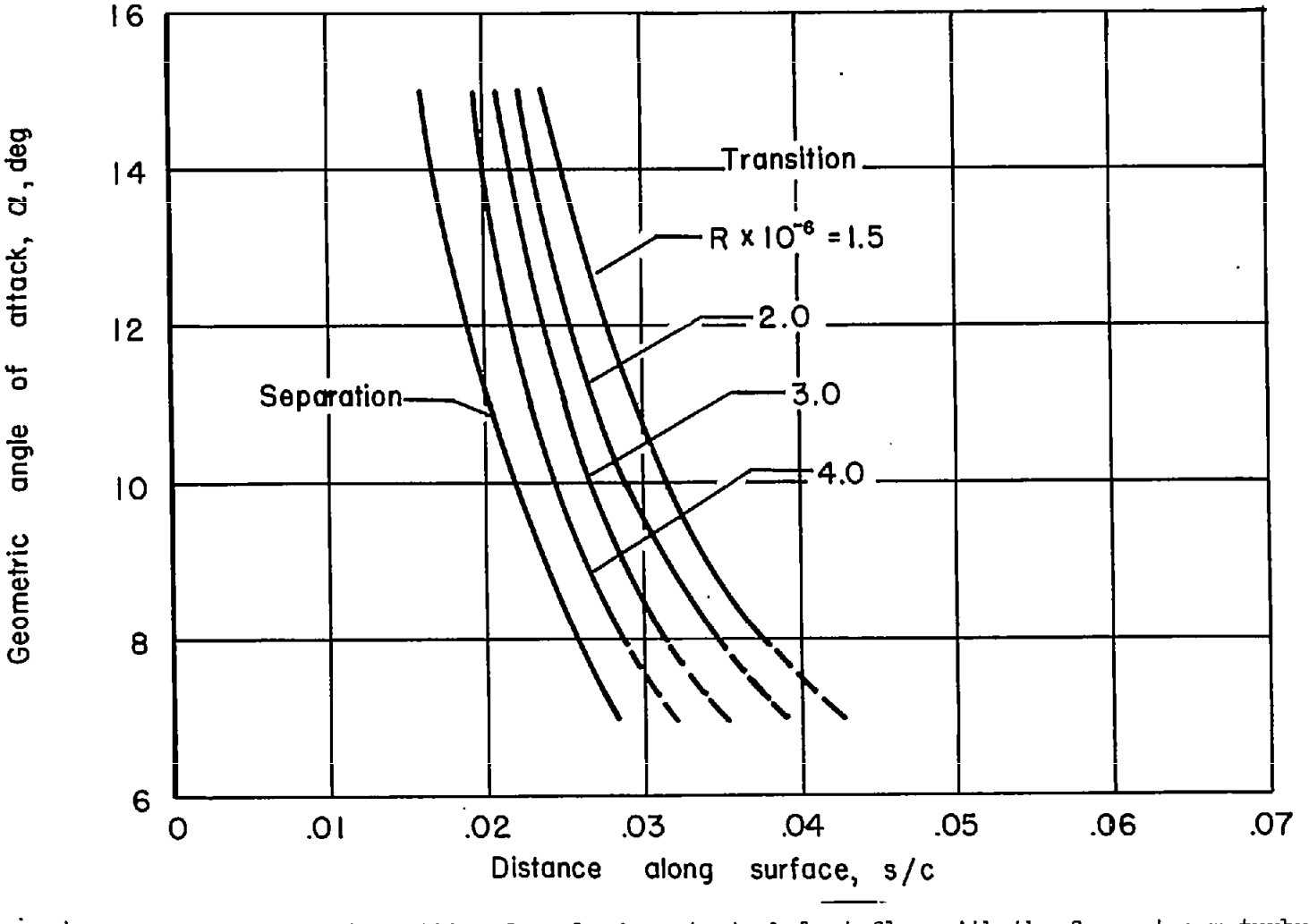

Figure 14.- The position of transition from laminar to turbulent flow with the free-stream turbulence increased to 1.10 percent; NACA 66_3-018 airfoil.

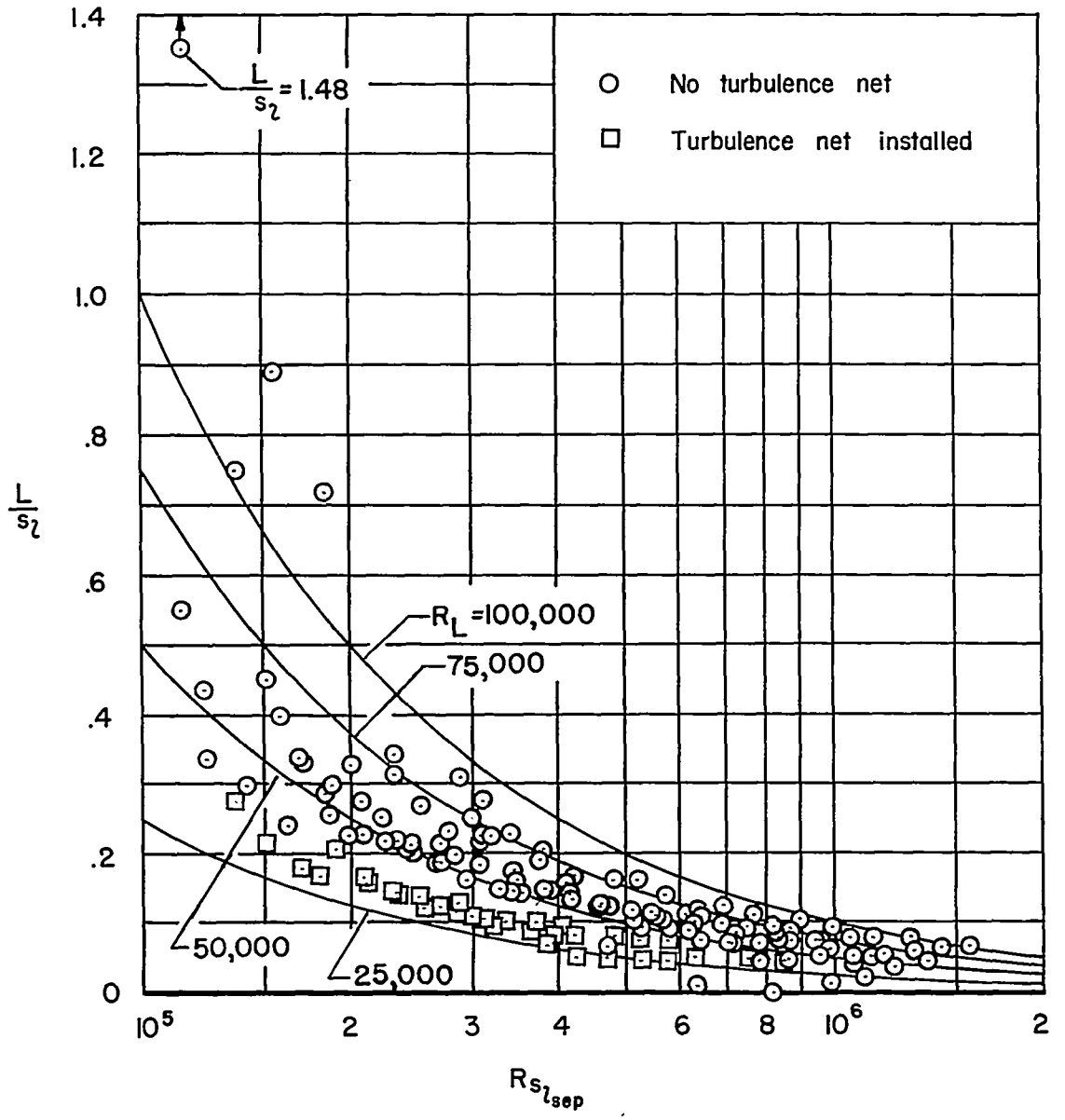

Figure 15.- Correlation of L/s_l with $R_{s_{l_{sep}}}$.

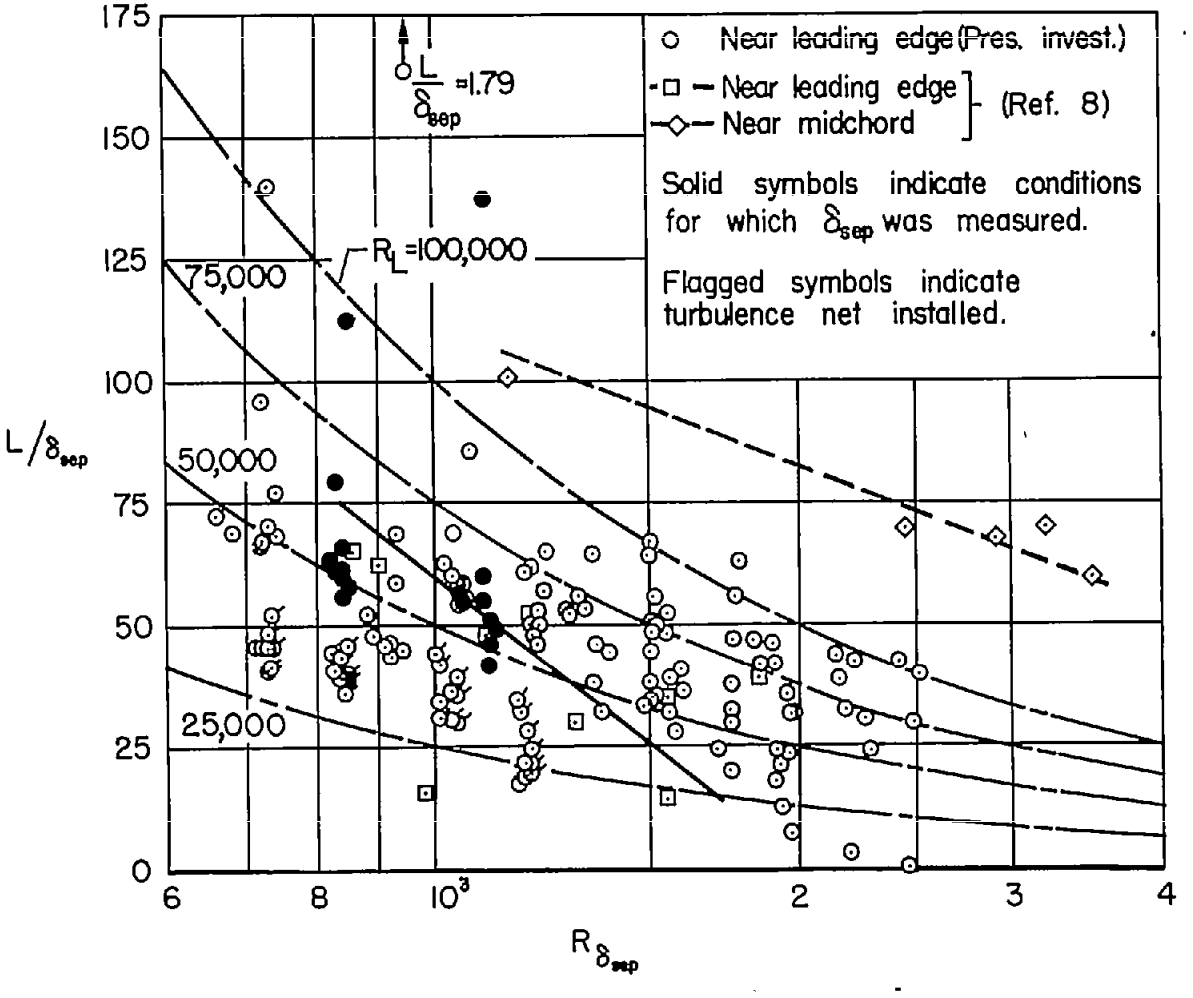

Figure 16.- Correlation of L/δ_{sep} with $R_{\delta_{sep}}$ as determined in present investigation and reference 8.

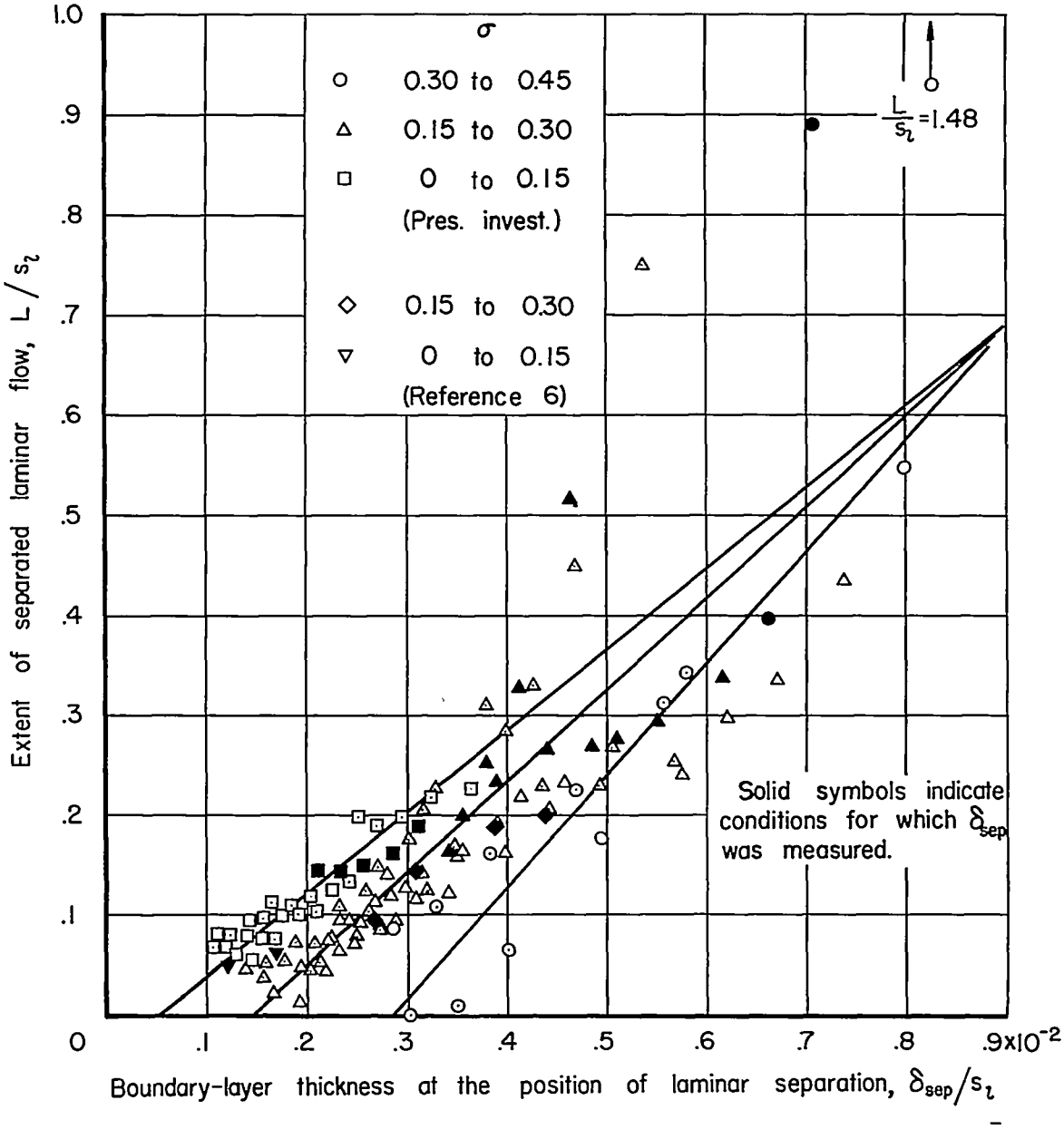

Figure 17.- Correlation of L/s_l with δ_{sep}/s_l and σ.

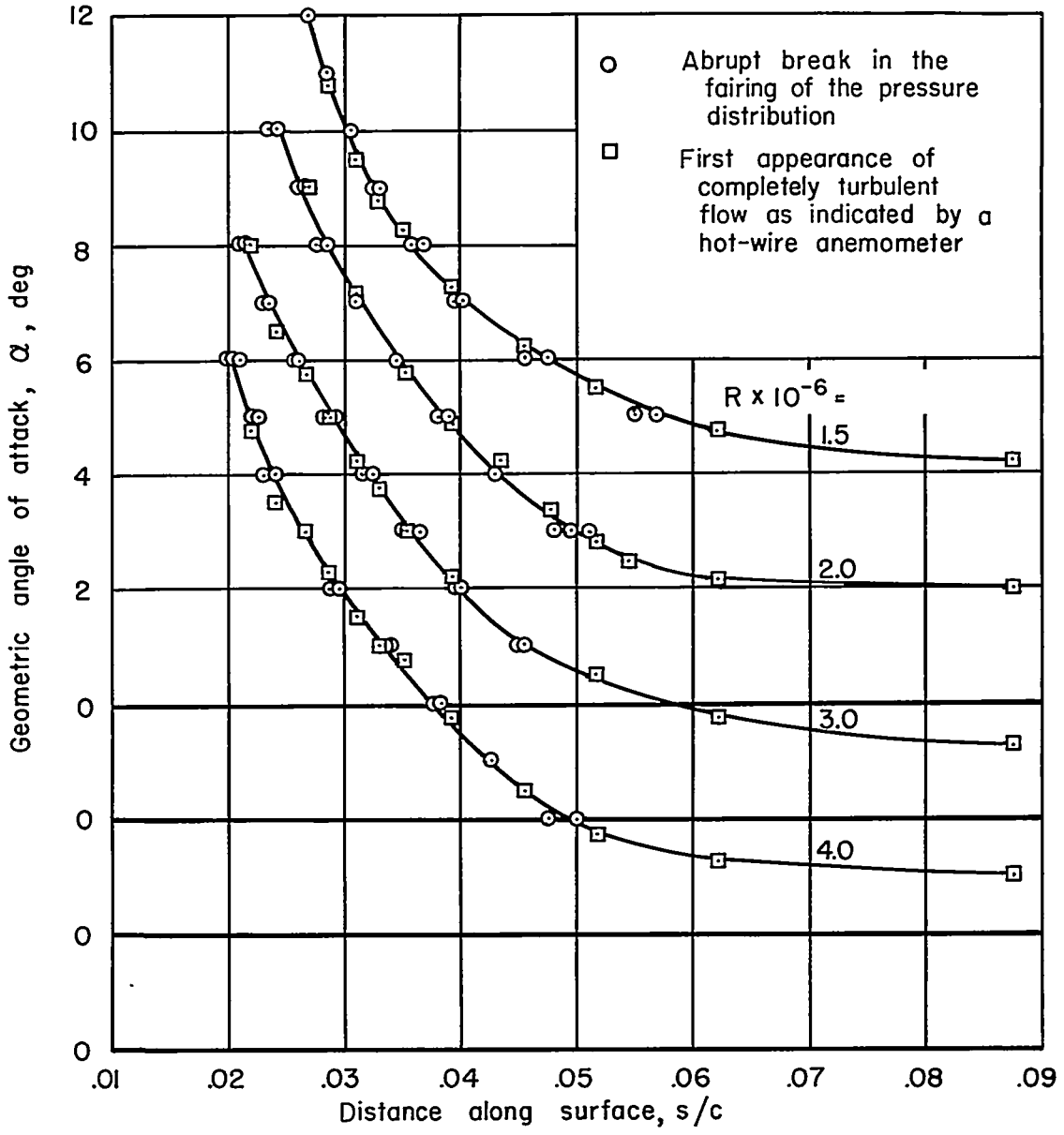

Figure 18.- Comparison between two methods for determining the position of transition from laminar to turbulent flow on the NACA 0010 (modified) airfoil.

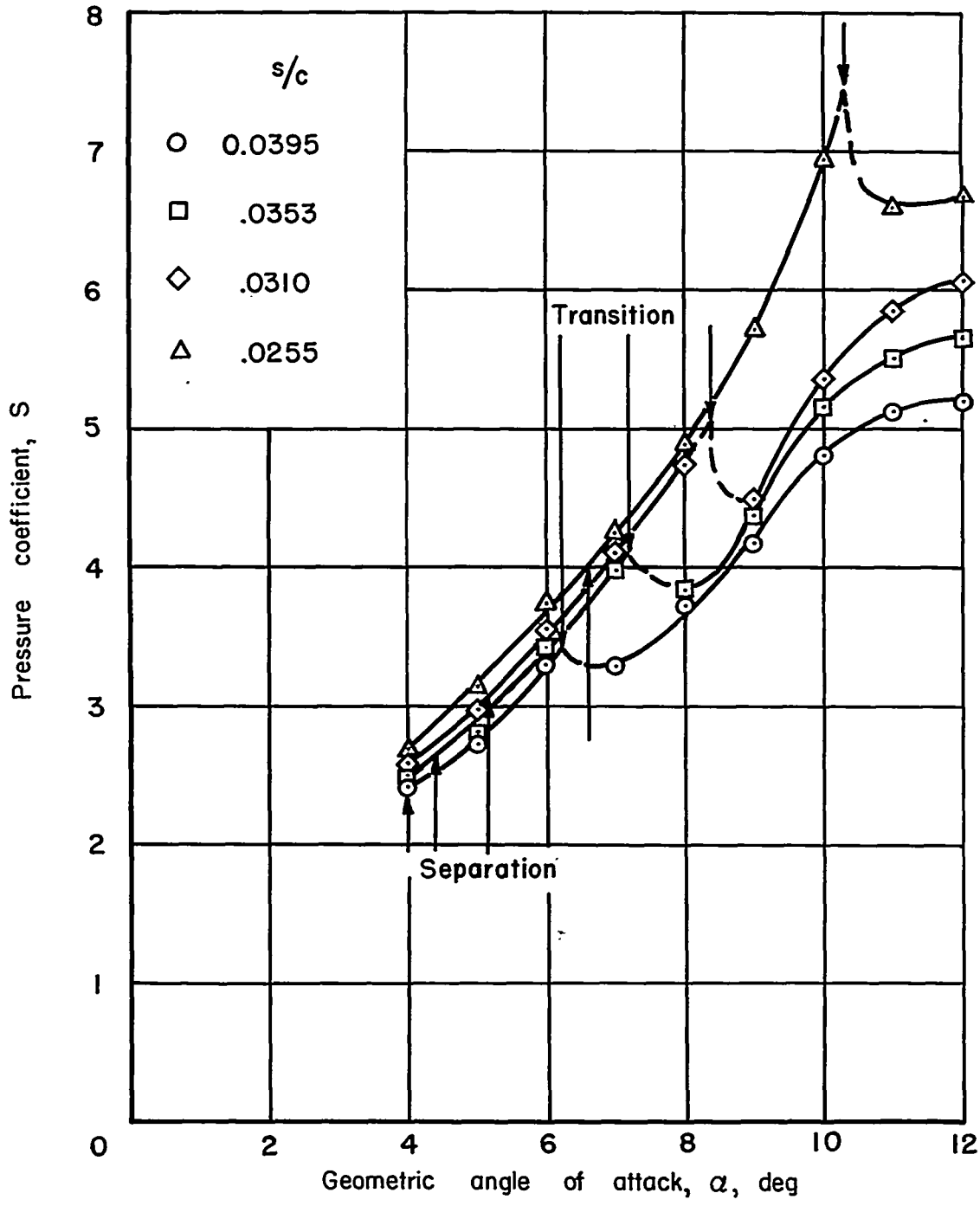

Figure 19.- The variation of the pressure coefficient with angle of attack for several chordwise stations on the NACA 0010 (modified) airfoil; $R = 3 \times 10^6$.

NACA - Langley Field, Va.